"In presenting the dissertation as a partial fulfillment of the requirements for an advanced degree from the Georgia Institute of Technology, I agree that the Library of the Institution shall make it available for inspection and circulation in accordance with its regulations governing materials of this type. I agree that permission to copy from, or to publish from, this dissertation may be granted by the professor under whose direction it was written, or, in his absence, by the dean of the Graduate Division when such copying or publication is solely for scholarly purposes and does not involve potential financial gain. It is understood that any copying from, or publication of, this dissertation which involves potential financial gain will not be allowed without written permission.

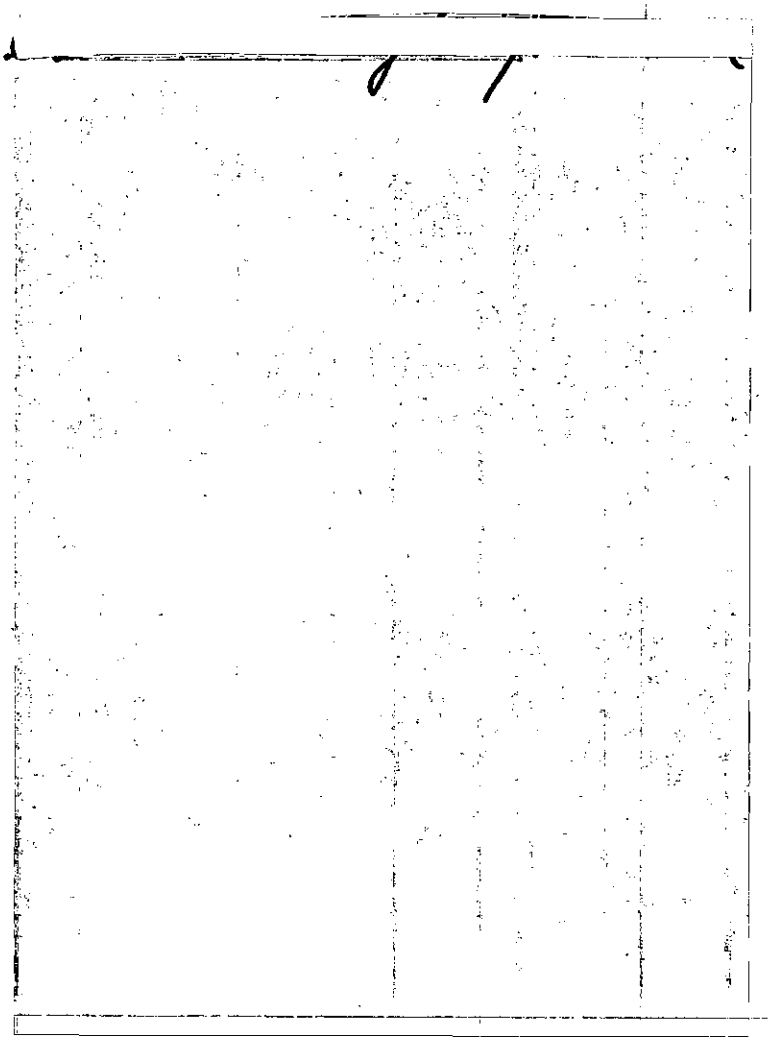

CENTRIFUGAL STRETCHING IN SYMMETRIC-TOP MOLECULES AND THE STARK EFFECT OF CHLOROTRIFLUOROMETHANE

A THESIS

Presented to

the Faculty of the Graduate Division

by

Richard Clayton Johnson

In Partial Fulfillment

of the Requirements for the Degree

Doctor of Philosophy in the School of Physics

Georgia Institute of Technology

June, 1961

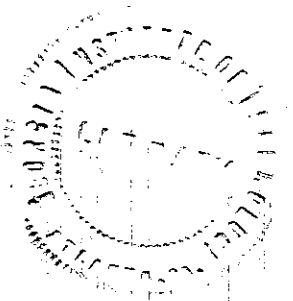

8a
12-a

CENTRIFUGAL STRETCHING IN SYMMETRIC-TOP MOLECULES AND THE STARK EFFECT OF CHLOROTRIFLUOROMETHANE

Approved:

Date Approved by Chairman: May 2, 1961

ACKNOWLEDGMENTS

The author is grateful to Drs. Thomas L. Weatherly and J. Q. Williams for their guidance and patience throughout this investigation. The advice and encouragement of Dr. Maurice W. Long is also appreciated. I am grateful to the Office of Naval Research and the National Science Foundation for supporting part of the investigation and to Mrs. Betty Lane for patiently typing this thesis.

TABLE OF CONTENTS

TABLE OF CONTENTS (Continued)

LIST OF TABLES

LIST OF ILLUSTRATIONS

LIST OF ILLUSTRATIONS (Continued)

SUMMARY

The effects of centrifugal distortion in symmetric-top molecules are usually predicted through the use of distortion constants, D_{JJ} and D_{JK}. It is expected that D_{JJ} will always be positive and that D_{JK} may be either positive or negative. Recently, CCl_3F and $CHCl_3$ were each reported to have a negative D_{JJ} which varies with the rotational quantum number J. This prompted further studies of distortion effects in other symmetric tops. Detailed calculations of distortion constants were made for three molecules: (a) CH_3Cl, a typical methyl halide; (b) $CClF_3$, a molecule with bonding similar to that of CCl_3F; and (c) CHF_3, a molecule with its center of mass within the CF_3 tetrahedron. All three were found to obey existing distortion theory within the limits of experimental error. The J = 1→2 through 4→5 transitions for $C^{12}Cl^{35}F_3$ were measured. Absorption lines for J = 2→3 and 3→4 have been reported previously; however, the 2→3 data are believed to be slightly in error. Present data yield B_o = 3335.596 mc, eqQ = -77.98 mc, D_{JJ} = +0.59 kc, and D_{JK} = +2.06 kc. Theoretical distortion constants can be calculated from the molecular structure and the molecular force constants. A comparison of measured and theoretical constants for nine symmetric-top molecules shows reasonable agreement for all except CCl_3F and $CHCl_3$, which are the only molecules considered having three identical nuclei with quadrupole moments. From Stark effect measurements on the J = 1→2 transition, the molecular dipole moment of $C^{12}Cl^{35}F_3$ was assigned the value 0.50 ± 0.01 debye.

CHAPTER I

INTRODUCTION

The effects of centrifugal distortion in symmetric-top molecules, neglecting electric quadrupole splitting, are usually predicted (1) through the use of two rotational distortion constants, D_{JJ} and D_{JK}. It has been surmised by some authors (2) that D_{JJ} will be positive for all symmetric tops, while D_{JK} may in principle be either positive or negative. It was pointed out that all molecules of the YZ_3 type which have so far been examined have D_{JK} negative, while molecules of the XYZ_3 type have D_{JK} positive.

A recent investigation (3, 4) on CCl_3F and $CHCl_3$ yielded negative values for both D_{JJ} and D_{JK}. In addition, it was found that D_{JJ} is a function of J for the low J-value data which were considered. Long (4) also pointed out that the centers of mass for previously reported XYZ_3 molecules are outside the YZ_3 tetrahedron and the centers of mass for CCl_3F, $CHCl_3$, and all YZ_3 molecules are within the YZ_3 tetrahedron.

The unexpected results of the above investigation (3, 4) invited further study of distortion effects in other symmetric tops. It was decided to calculate distortion effects of $CClF_3$ in detail because the bonding is similar to that of CCl_3F. In addition, it was decided to compare the results with those of CH_3Cl, a typical methyl halide, and of CHF_3, a molecule with its center of mass toward the base of the YZ_3 tetrahedron. It was found that all three molecules can be described,

within the limits of experimental errors, by existing rotational distortion theory (i.e., the distortion constants D_{JJ} and D_{JK} are not functions of J or K).

The theoretical rotational distortion constants, D_{JJ} and D_{JK}, can be calculated (5, 6) from the molecular structure and the molecular force constants; the former is calculated from microwave spectra and the latter are calculated from Raman and infrared spectra. A comparison of the theoretical and observed distortion constants for nine symmetric-top molecules provided an interesting link between spectra in the microwave and infrared regions. There was reasonable agreement for all except CCl_3F and $CHCl_3$, the only molecules considered which have three identical nuclei with quadrupole moments. The disagreement was serious in these two cases.

The electric dipole moment of $CClF_3$ was evaluated by Birnbaum (7) using a cavity method to determine the nonresonant, or Debye type, absorption. It was later evaluated by Beeson (8) by measuring and analyzing the Stark effect for the $J = 2 \rightarrow 3$ transition. The latter determination was not considered very accurate because of difficulty in resolving the Stark components. It was decided to evaluate the dipole moment by measuring and analyzing the Stark effect for the $J = 1 \rightarrow 2$ transition since the Stark spectrum is considerably less complex for this transition.

CHAPTER II

INSTRUMENTATION

The microwave spectrometer used in this investigation is illustrated in the simplified block diagram of Figure 1. It is a Stark modulation type similar to that introduced by Hughes and Wilson (9).

Basically, the equipment consists of a klystron with power supply, a Stark cell, and a crystal detector. Absorption of the gas is modulated by a zero based, 85 kc, square wave, Stark generator, and the signal is amplified by an 85 kc amplifier. A phase sensitive detector is used to reduce effective bandwidth and to distinguish absorption lines from the Stark components.

When using an oscilloscope display, as illustrated in Figure 1, the klystron frequency, the display oscilloscope, and the power monitor oscilloscope are swept in synchronism. The absorption lines appear as upward displacements and the Stark components appear as downward displacements. When the setting of the cavity wavemeter is within the band of frequencies swept by the klystron, the wavemeter frequency appears as a dip on the power monitor oscilloscope; it can be used to determine the absorption line frequency within a few megacycles.

The absorption line frequency is accurately determined through the use of a fixed marker generator, whose oscillator is adjusted to zero beat with the National Bureau of Standards Station, WWV. The generator produces a family of markers spaced every 30 mc apart; its output is mixed with a sample of the klystron signal and the beat frequency is

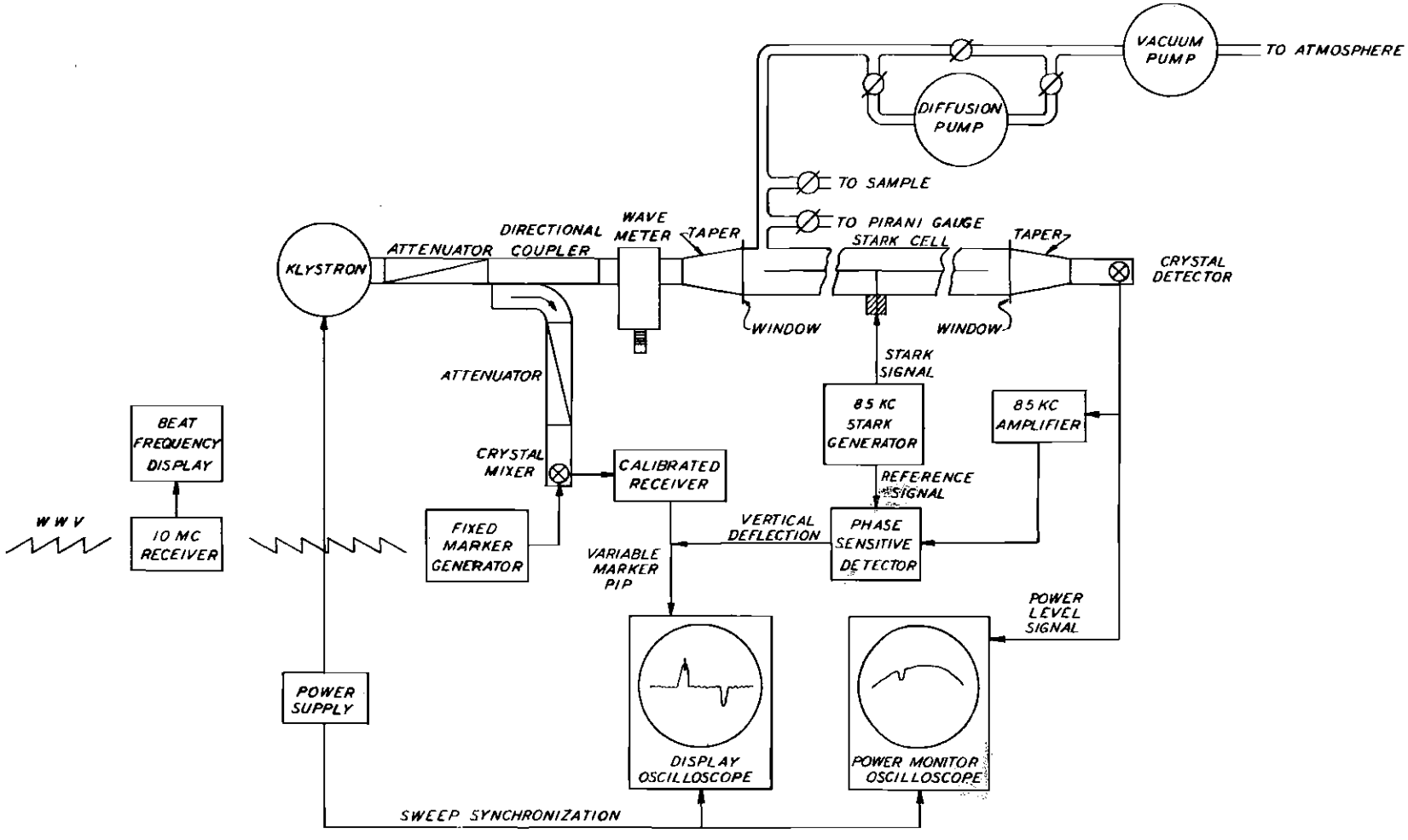

Figure 1. Simplified Block Diagram of the Stark Effect Microwave Spectrometer.

measured by a calibrated National HRO receiver. When the beat frequency corresponds to the setting of the calibrated receiver, a marker pip appears on the display oscilloscope. By tuning the calibrated receiver, the marker pip can be varied until it is superimposed on the absorption line being measured. The frequency of the absorption line is then determined by adding (or subtracting) the calibrated receiver frequency to the appropriate fixed marker frequency, as determined by the wavemeter. Several measurements are made as the klystron is swept from low to high frequencies, and then several measurements are made while sweeping from high to low frequencies. These measurements are averaged in order to eliminate errors due to time delays or nonlinearities in the sweep circuits.

The klystron frequency can be swept slowly through the use of a variable, low speed, mechanical drive mechanism, while the signal from the phase sensitive detector is displayed on an Easterline-Angus recorder. With this slow sweep, a very large filter time constant can be used in the output of the phase sensitive detector, thereby reducing effective bandwidth and increasing signal-to-noise ratio.

Either of two Stark cells is available for use, depending upon the operating frequency. The X-band cell has inside cross-sectional dimensions 0.900 inch by 0.400 inch and a length of 17 feet; the S-band cell has inside cross-sectional dimensions 2.84 inches by 1.34 inches and a length of 12 feet. The operating frequencies are approximately 8.2 to 45 kmc for the X-band cell and 2.6 to 16 kmc for the S-band cell. Both cells have a brass Stark electrode which is supported by insulating strips of teflon along the inner wall of each side of the waveguide. In

this manner, the applied Stark field is parallel to the electric field of the incident microwave energy. Each cell is housed in a wooden framework lined with polyfoam which serves as an insulator to facilitate cooling the cell with dry ice.

A small quantity of the sample gas is admitted into the Stark cell through a stopcock on the manifold of the vacuum system. An oil diffusion pump followed by a mechanical vacuum pump is used to pump the gas out of the system until the desired operating pressure is reached, as indicated by a Pirani gauge.

CHAPTER III

SYMMETRIC-TOP MOLECULES

The moments of inertia of a molecule (or any rigid system of masses) may be represented by an ellipsoid whose orientation is fixed in the molecule and whose center coincides with the center of mass. If the coordinate system is oriented so that x, y, and z are along the principal axes of the ellipsoid of inertia, the equation for the ellipsoid may be written as

$$x^2 I_{xx} + y^2 I_{yy} + z^2 I_{zz} = 1 \quad , \tag{1}$$

where I_{xx}, I_{yy}, and I_{zz} are the moments of inertia along the principal axes. The moment of inertia about any other axis is equal to the square of the reciprocal of the radius vector from the origin to the ellipsoid of inertia measured along the axis of interest. The three principal moments of inertia are usually arranged in increasing order of size and designated I_A, I_B, and I_C. In the most general case, all three moments of inertia are different, $I_A < I_B < I_C$, and the molecule is called an asymmetric top. In the case where two of the moments of inertia are equal and different from the third, the molecule is called a symmetric top. The prolate type has $I_A < I_B = I_C$ (momental ellipsoid elongated along the symmetry axis), and the oblate type has $I_A = I_B < I_C$ (momental ellipsoid flattened along the symmetry axis). Usually the z-axis is chosen along the symmetry axis. Then, I_A and I_C are the moments of inertia along the

symmetry axis for prolate and oblate tops, respectively, and I_B is the moment of inertia about an axis through the center of mass and perpendicular to the symmetry axis.

Rigid Rotor

The quantized rotational energy levels for a rigid symmetric-top molecule were first obtained by Dennison (10) with matrix mechanical methods and later by Reiche and Rademaker (11) and by Kronig and Rabi (12) with the Schrodinger Equation. The quantized energies for a prolate top can be expressed as

$$W = \frac{J(J+1)h^2}{8\pi^2 I_B} + \left(\frac{h^2}{8\pi^2 I_A} - \frac{h^2}{8\pi^2 I_B}\right) K^2 \quad . \tag{2}$$

By defining the rotational constants

$$A = \frac{h}{8\pi^2 I_A} \quad \text{and} \quad B = \frac{h}{8\pi^2 I_B} \quad , \tag{3}$$

Equation 2 can be written

$$\frac{W}{h} = J(J+1)B + K^2(A-B) \quad , \tag{4}$$

where h is Planck's constant, J is the rotational angular momentum quantum number, and K is the quantum number specifying the component of rotational angular momentum along the molecular symmetry axis. For an oblate top, the rotational constant A is replaced by C, where

$$C = \frac{h}{8\pi^2 I_C} \quad . \tag{5}$$

In microwave spectroscopy, rotational constants are most often expressed in megacycles. Therefore, W/h in Equation 4 expresses the quantized energies in units of megacycles.

The quantum mechanical treatment of the symmetric top involves three quantum numbers,

$$\begin{aligned} J &= 0, 1, 2, \ldots \\ K &= 0, \pm 1, \pm 2, \ldots, \pm J \\ M_J &= 0, \pm 1, \pm 2, \ldots, \pm J \quad , \end{aligned} \tag{6}$$

which have the following significance. The total rotational angular momentum has the magnitude $\sqrt{J(J+1)}\hbar$, the z-component of rotational angular momentum is $K\hbar$, and the Z-component of rotational angular momentum is $M_J\hbar$, where $\hbar = h/2\pi$. Figure 2 illustrates the vector relations of rotational angular momenta for a symmetric-top molecule. Selection rules for the symmetric rotor, involving no quadrupole interaction, are

$$\begin{aligned} \Delta J &= 0, \pm 1 \\ \Delta K &= 0 \\ \Delta M_J &= 0, \pm 1 \quad . \end{aligned} \tag{7}$$

For an absorption transition with the Stark field parallel to the electric field of the microwave radiation, the selection rules for J and M_J are

$$\begin{aligned} \Delta J &= +1 \\ \Delta M_J &= 0 \quad . \end{aligned}$$

In the absence of an external field, the selection rule for M_J is unimpor-

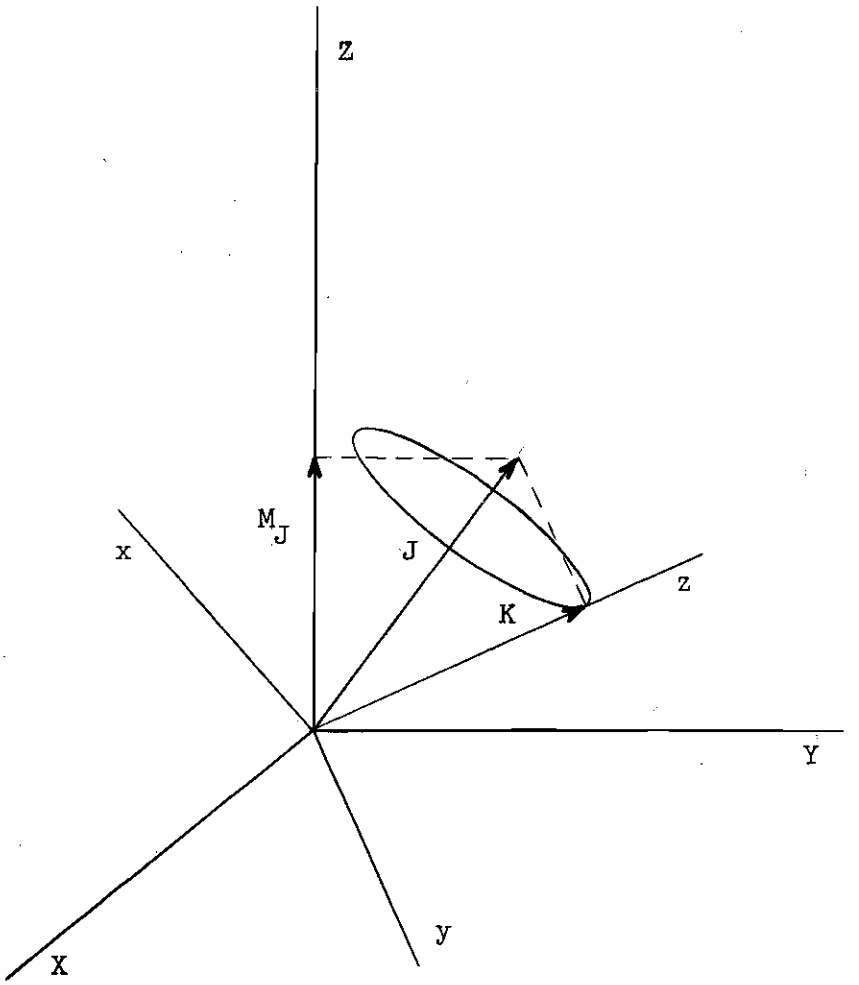

Figure 2. Vector Relations of Rotational Angular Momenta for a Symmetric-Top Molecule. The XYZ system is fixed in space, and the xyz system is fixed in the molecule with z along the symmetry axis.

tant since the rotational energy expressed in Equation 2 is independent of M_J.

Centrifugal Stretching

The above discussion is applicable to a rigid molecule. When the effects of centrifugal distortion are included (1), the quantized energy levels can be expressed as

$$\frac{W}{h} = J(J+1)B + K^2(A-B) - J^2(J+1)^2D_{JJ} - J(J+1)K^2D_{JK} - K^4D_{KK} \quad (8)$$

where D_{JJ}, D_{JK}, and D_{KK} represent distortion constants which are small compared with A or B.

The absorption frequency resulting from a rotational transition $J \rightarrow J+1$ and $\Delta K = 0$ is

$$\nu = 2(J+1)B - 4(J+1)^3D_{JJ} - 2(J+1)K^2D_{JK} \quad . \quad (9)$$

For a rigid molecule, the absorption lines are equally spaced; and for a given transition of J, all possible values of K give identical frequencies. For a nonrigid molecule, the degeneracy is removed because of the D_{JK} distortion constant, as may be seen in Equation 9. A high-resolution microwave spectroscope can usually resolve the lines involving different K's, so that D_{JK} can be evaluated.

Quadrupole Hyperfine Structure

For most molecules in the electronic ground state, the magnetic fields produced by various electronic orbitals almost completely cancel,

resulting in zero or a very small magnetic field at the nucleus and therefore a negligible hyperfine structure. However, the electric quadrupole interactions in molecules may give rise to a sizable hyperfine structure.

If the electric charge of a nucleus is not spherically symmetric, which is usually the case when the nuclear spin $I \geq 1$, the nucleus has an electric quadrupole moment Q which can couple the nuclear axis to the molecular framework by interaction with the average electric field gradient of the molecule at the nucleus. Vectorially, the nuclear spin angular momentum $\vec{I}$ and the rotational angular momentum $\vec{J}$ can be regarded as forming a resultant total angular momentum $\vec{F}$, fixed in space, about which both $\vec{I}$ and $\vec{J}$ precess. The vector relations of angular momenta for a symmetric-top molecule with IJ-coupling are illustrated in Figure 3. The quantum conditions on F and M_F are

$$F = J + I,\ J + I - 1,\ \ldots,\ |J - I| \qquad (10)$$
$$M_F = 0,\ \pm 1,\ \pm 2,\ \ldots,\ \pm F \quad ,$$

and the quantum number I is fixed for a particular nucleus. The nuclear spin angular momentum has the magnitude $\sqrt{I(I+1)}\hbar$, the total angular momentum has the magnitude $\sqrt{F(F+1)}\hbar$, and the Z-component of total angular momentum is $M_F\hbar$.

The nuclear quadrupole energy, expressed in units of frequency, for a nucleus on the molecular axis of a symmetric top can be expressed as (13)

$$\frac{W_Q}{h} = eqQ\ f(I,J,F)\ g(J,K) \quad , \qquad (11)$$

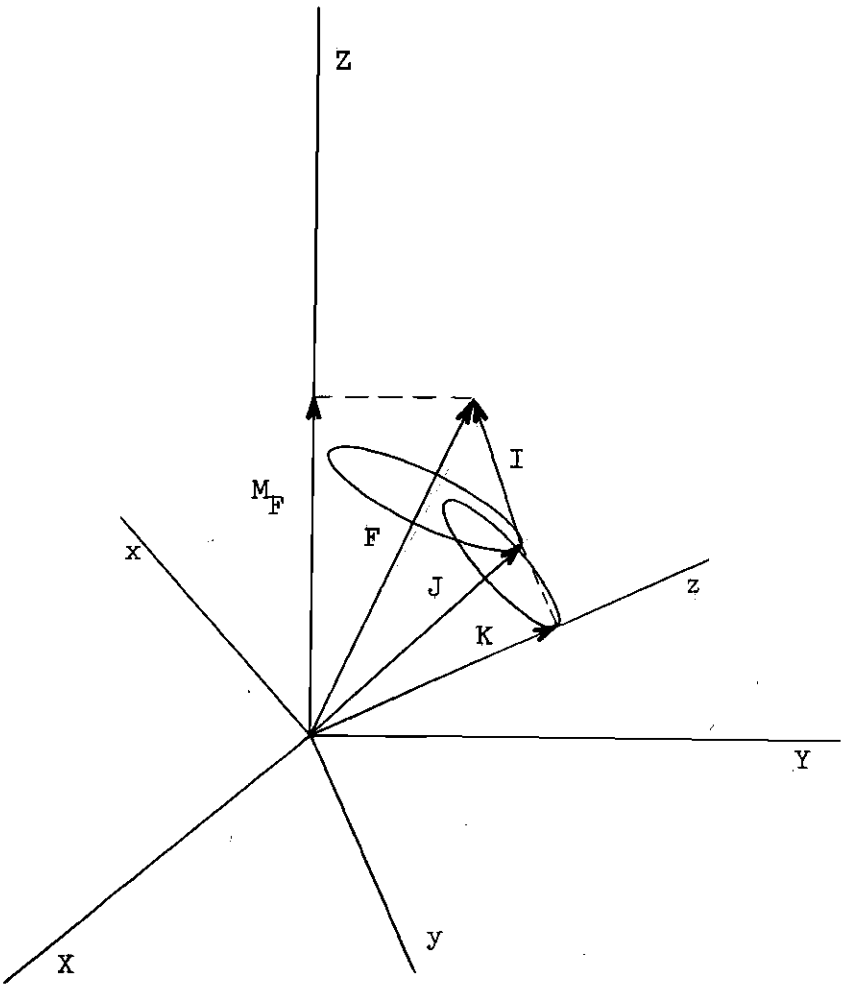

Figure 3. Vector Relations of Angular Momenta for a Symmetric-Top Molecule With IJ-Coupling. The XYZ system is fixed in space, and the xyz system is fixed in the molecule with z along the symmetry axis.

where e is the charge of one proton, q is the second partial derivative of the electric potential (resulting from extranuclear charges) with respect to the molecular symmetry axis evaluated at the nucleus considered, Q is the electric quadrupole moment of the nucleus, and

$$f(I,J,F) = \frac{(3/4)C(C+1) - I(I+1)J(J+1)}{2I(2I-1)(2J-1)(2J+3)} \tag{12}$$

$$C = F(F+1) - I(I+1) - J(J+1)$$

$$g(J,K) = \frac{3K^2}{J(J+1)} - 1 \quad . \tag{13}$$

The quantity eqQ is called the quadrupole coupling constant. A table of Casimir's function, f(I,J,F), and relative intensities of hyperfine components (14) is helpful when calculating energies resulting from nuclear quadrupole interactions.

Rotational Spectra

In the above discussion, three kinds of energy in a rotating symmetric-top molecule have been considered. In order of decreasing magnitude, they are (a) rotational energy, (b) quadrupole coupling energy, and (c) distortion energy. The latter is closely related to rotational energy.

In a rotational absorption transition, the molecule goes from an initial state to a final state, each of which can be specified by the quantum numbers J, K, I, and F. The selection rules for a symmetric top, not involving quadrupole interaction, are given in Equation 7; selection rules for a symmetric top having quadrupole interaction are

$$\Delta J = 0, \pm 1 \qquad (14)$$
$$\Delta K = 0$$
$$\Delta I = 0$$
$$\Delta F = 0, \pm 1$$
$$\Delta M_F = 0, \pm 1 \quad .$$

For an absorption transition with the Stark field parallel to the electric field of the microwave radiation, the selection rules for J and M_F are

$$\Delta J = +1$$
$$\Delta M_F = 0 \quad .$$

The absorption frequency is determined by the difference between the initial and final state energies. Let the following definitions apply to the energy differences expressed in megacycles:

- ν absorption line frequency,
- ν_R rotational energy difference which assumes a rigid molecule,
- ν_D distortion energy correction term which accounts for a nonrigid molecule, and
- ν_Q quadrupole energy term which accounts for the interaction between the nuclear quadrupole moment and the average field gradient at the nucleus.

The absorption frequency for the transition $J \rightarrow J+1$, $\Delta K = 0$, $F_i \rightarrow F_f$ (i and f refer to initial and final states) is

$$\nu = \nu_R + \nu_D + \nu_Q \quad , \qquad (15)$$

where

$$\nu_R = 2(J+1)B \tag{16}$$

$$\nu_D = -4(J+1)^3 D_{JJ} - 2(J+1)K^2 D_{JK} \tag{17}$$

$$\nu_Q = eqQ \left[g(J+1,K)\ f(I,J+1,F_f) - g(J,K)\ f(I,J,F_i) \right] . \tag{18}$$

The functions f and g are defined in Equations 12 and 13.

Analysis of Microwave Data

Referring to Equations 15 through 18, one sees that it is necessary to evaluate four constants; they are the rotational constant B, the distortion constants D_{JJ} and D_{JK}, and the quadrupole coupling constant eqQ. The various terms of Equation 15 are functions of the quantum numbers, as indicated in the following:

$$\nu(J,K,I,F_i,F_f) = \nu_R(J) + \nu_D(J,K) + \nu_Q(J,K,I,F_i,F_f) . \tag{19}$$

Assume that as many lines as possible have been measured and identified by the quantum numbers of the initial and final states. Evaluation of the constants can proceed as follows.

Quadrupole Coupling Constant, eqQ.--To evaluate the quadrupole coupling constant, choose a group of lines involving the same J and K, but different combinations of F_i and F_f. Designate lines by numerical subscripts; then a pair (e.g., numbers 1 and 2) can be used as follows:

$$\nu_1 = \nu_R(J) + \nu_D(J,K) + \nu_Q(J,K,I,F_{i1},F_{f1})$$

$$\nu_2 = \nu_R(J) + \nu_D(J,K) + \nu_Q(J,K,I,F_{i2},F_{f2}) .$$

Subtracting gives

$$\Delta\nu_{12} = \nu_1 - \nu_2 = \nu_Q(J,K,I,F_{i1},F_{f1}) - \nu_Q(J,K,I,F_{i2},F_{f2})$$

or

$$eqQ = \Delta\nu_{12} \div \left\{\left[g(J+1,K)\ f(I,J+1,F_{f1}) - g(J,K)\ f(I,J,F_{i1})\right] - \left[g(J+1,K)\ f(I,J+1,F_{f2}) - g(J,K)\ f(I,J,F_{i2})\right]\right\} \quad . \tag{20}$$

If the constant eqQ is evaluated for every possible pair of lines in each group involving the same J and K, a weighted average can be taken and assigned as the quadrupole coupling constant, eqQ, for the molecule. If it is assumed that each line is measured with identical accuracy, then $\Delta\nu$ is a reasonable weighting factor. A faulty frequency measurement can often be detected by examining the "spread" of the individual calculations.

Distortion Constant, D_{JK}.--After the quadrupole coupling constant has been evaluated, the quadrupole energy contribution ν_Q to each line can be calculated. Define the unsplit line frequency as

$$\nu' = \nu - \nu_Q = \nu_R + \nu_D \quad . \tag{21}$$

If the unsplit line frequency is calculated for each measured absorption line, a weighted value can be assigned to each group involving the same J and K. This is the theoretical frequency that would be observed if quadrupole coupling were not present. A logical weighting factor is the relative line intensity.

Equation 21 can be written as

$$\nu' = 2(J+1)B - 4(J+1)^3D_{JJ} - 2(J+1)K^2D_{JK}$$

or

$$\frac{\nu'}{2(J+1)} = B - 2(J+1)^2 D_{JJ} - K^2 D_{JK} \quad . \tag{22}$$

Evaluate $\nu'/2(J+1)$ for each unsplit line frequency; choose pairs involving the same J but different K (designated by numerical subscripts, e.g., 1 and 2). From Equation 22,

$$\frac{\nu'_1}{2(J+1)} = B - 2(J+1)^2 D_{JJ} - K_1^2 D_{JK}$$

$$\frac{\nu'_2}{2(J+1)} = B - 2(J+1)^2 D_{JJ} - K_2^2 D_{JK} \quad .$$

Subtracting the above equations, the distortion constant is found to be

$$D_{JK} = \frac{\frac{\nu'_1}{2(J+1)} - \frac{\nu'_2}{2(J+1)}}{K_2^2 - K_1^2} \quad . \tag{23}$$

If estimated errors have been assigned to each unsplit line frequency, then estimated errors can be assigned to each calculation of D_{JK}, and a weighted average can be taken for the molecule. A logical weighting factor is the reciprocal of the estimated error for each calculation.

Distortion Constant, D_{JJ}.--The evaluation of the distortion constant D_{JJ} is similar to that for D_{JK}. After $\nu'/2(J+1)$ has been evaluated for each unsplit line frequency, choose pairs involving the same K but different J (designated by numerical subscripts, e.g., 1 and 2). From Equation 22,

$$\frac{\nu'_1}{2(J_1+1)} = B - 2(J_1+1)^2 D_{JJ} - K^2 D_{JK} \quad ,$$

and

$$\frac{\nu_2'}{2(J_2+1)} = B - 2(J_2+1)^2 D_{JJ} - K^2 D_{JK} \quad .$$

Subtracting the above equations, the distortion constant is found to be

$$D_{JJ} = \frac{\frac{\nu_1'}{2(J_1+1)} - \frac{\nu_2'}{2(J_2+1)}}{2(J_2+1)^2 - 2(J_1+1)^2} \quad . \tag{24}$$

Estimated errors can be assigned for each calculation as they were for D_{JK} and a weighted average can be taken for the molecule.

Rotational Constant, B.--After the quadrupole coupling constant and distortion constants have been evaluated, the rotational energy difference,

$$\nu_R = \nu - \nu_Q - \nu_D \quad , \tag{25}$$

can be evaluated for each measured line, and an average value can be taken for those involving the same J. The rotational constant can then be evaluated for each J transition by

$$B = \frac{\nu_R}{2(J+1)} \quad . \tag{26}$$

If estimated errors have been assigned to each rotational energy difference, then estimated errors can be assigned to each calculation of B, and a weighted average can be taken for the molecule.

Molecular Models

Some authors attempt to explain the magnitude and algebraic sign of measured distortion constants by referring to simple molecular models.

Most arguments, however, which attempt to give the reader a simple "picture" of what is happening, are incomplete and therefore unacceptable. To be complete, the model must be capable of predicting energy levels for each quantum state; then from the calculation of allowed transition frequencies between states, the distortion constants can be evaluated. The energy levels should include the total energy--the kinetic energy due to rotation about both axes and the potential energy which is stored in the stretched bonds. Arguments which do not include total energy are not acceptable.

In the course of a discussion concerning the positive value of D_{JK} for methyl halides, Thomas, Cox, and Gordy (16) suggested a method whereby D_{JJ} might be negative. The argument, which concerns hybridization of the bonding orbitals, is as follows. An increase in angular momentum about the symmetry axis tends to make the CH_3 group more nearly planar, and hence to increase the S character in the three C orbitals which bond to hydrogen. For a completely planar structure, each of these orbitals would have 33 per cent S character; whereas, the usual tetrahedral bonding has 25 per cent S character (see Appendix D). As a consequence, the C orbital bonding to the halogen must be reduced for proper normalization. This tends to make the C-H bonds stronger, the C-Hal bond weaker, and D_{JK} positive. By similar arguments, one might conclude that end over end rotation, because it tends to decrease the H-C-H angle (see Appendix C), will decrease the S character of the C-H bonds and consequently increase the S character of the C-Hal bond; this tends to make the C-Hal bond stronger and D_{JJ} negative. The argument is interesting because it suggests the possibility of a negative D_{JJ};

however, the argument is incomplete because it does not consider the kinetic energy due to rotation about the symmetry axis and the potential energy stored in the bonds.

A more satisfactory approach for calculating distortion constants theoretically was undertaken by Slawsky and Dennison (1). They applied the theory of the semi-rigid rotor, which was developed by Wilson and Howard (18), to the symmetric molecules YZ_3 and XYZ_3. It was found that the change in rotational energy, caused by centrifugal distortions, can be expressed in terms of the quantum numbers J and K and as a function of the potential constants and the molecular dimensions. More recently, the calculation of rotational distortion constants for some axially symmetric XYZ_3 molecules was considered by Dowling, Gold, and Meister (5, 6). Explicit equations were written for the rotational distortion constants D_{JJ}, D_{JK}, and D_{KK} in terms of the masses, internuclear distances, interbond angles, and the molecular force constants. This method is discussed further in the next chapter.

CHAPTER IV

ROTATIONAL DISTORTIONS IN SYMMETRIC-TOP MOLECULES

Effects of centrifugal distortion in symmetric-top molecules, neglecting electric quadrupole splitting, are expressed by the distortion constants D_{JJ} and D_{JK} in the equation,

$$\frac{\nu}{2(J+1)} = B - 2(J+1)^2 D_{JJ} - K^2 D_{JK} \quad , \tag{27}$$

for a transition $J \rightarrow J+1$ and $\Delta K = 0$. It has been surmised by some authors (2) that D_{JJ} will be positive for all symmetric tops, while D_{JK} may in principle be either positive or negative. It was also pointed out that all molecules of the type YZ_3 which have so far been examined have D_{JK} negative, while molecules of the type XYZ_3 have D_{JK} positive.

A recent investigation (3, 4) of CCl_3F and $CHCl_3$ yielded negative values for both D_{JJ} and D_{JK}. In addition, it was found that D_{JJ} is a function of J for the low J-value data which were considered. Long (4) also pointed out that the centers of mass for previously reported XYZ_3 molecules are outside the YZ_3 tetrahedron, and the centers of mass for CCl_3F, $CHCl_3$, and YZ_3 molecules are within the YZ_3 tetrahedron. It has since been pointed out that CHF_3 has its center of mass within the YZ_3 tetrahedron and was reported (15) to have D_{JJ} positive and D_{JK} negative. A search, in conjunction with M. W. Long, for reported values of D_{JK}, for YZ_3 and XYZ_3 molecules, yielded two distinct groups. Group I has the center of mass outside the YZ_3 tetrahedron and D_{JK} positive, while

Group II has the center of mass within the YZ_3 tetrahedron and D_{JK} negative.

	Group I	
CH_3Br	$CClF_3$	F_3GeCl
CH_3Cl	CF_3I	PF_3S
CH_3F	H_3BCO	SiF_3Cl
CH_3I	H_3CCCI	SiF_3Br
$CBrF_3$	F_3CCCH	
	Group II	
$CHCl_3$	NH_3	PH_3
CHF_3	ND_3	AsF_3
CCl_3F		

It is interesting to note that the signs of D_{JK} calculated later (see Table 5) also agree with this grouping.

The unexpected results of Long's work concerning distortion constants of CCl_3F and $CHCl_3$ invited further investigations of the subject. It was decided to study distortion effects of $CClF_3$ in detail because the bonding is similar to that of CCl_3F. Since the center of mass for this molecule is outside the YZ_3 tetrahedron, it was expected that D_{JK} would be positive. In addition, it was decided to compare the results with those of CH_3Cl, a typical methyl halide, and of CHF_3, a molecule with its center of mass toward the base of the YZ_3 tetrahedron.

Chloromethane, CH_3Cl

The microwave absorption spectrum of methyl chloride (chloromethane) has been analyzed and reported by Thomas, Cox, and Gordy (16). The

resolved hyperfine lines, reported in Reference 16, for the J = 3→4 and J = 5→6 transitions were used to calculate distortion constants for all possible combinations of the hypothetical unsplit lines. The results are illustrated in Figures 4 and 5. It was necessary to select an arbitrary estimated error for the unsplit lines of only ±0.03 mc in order to have good agreement among the various calculations of D_{JJ} and D_{JK}. This estimated error is quite low considering that the line frequencies were approximately 106 kmc and 159 kmc.

The weighted averages, based on this author's calculations, are

$$D_{JJ} = + 17.7 \text{ kc}$$

and

$$D_{JK} = + 198.5 \text{ kc} \quad ;$$

whereas, the values reported by Thomas, Cox, and Gordy are

$$D_{JJ} = + 18.1 \pm 0.5 \text{ kc}$$

and

$$D_{JK} = + 198.0 \pm 5.0 \text{ kc} \quad .$$

It is possible that the values reported by Thomas, Cox, and Gordy are based on additional data. This author's calculations were made to see if the individual D_{JJ} and D_{JK} calculations were consistent.

Chlorotrifluoromethane, $CClF_3$

The microwave absorption spectrum of chlorotrifluoromethane has been reported for the J = 2→3 and J = 3→4 transitions by Coles and Hughes (17). Using their data, the distortion constants D_{JJ} and D_{JK} were calculated for all combinations of hypothetical unsplit line frequencies.

		J = 3→4				J = 5→6				
	K	0	1	2	3	0	1	2	3	4
J = 3→4	0		198.0 ±7.5	199.5 ±1.9	198.7 ±0.8	17.7 ±0.2				
	1	198.0 ±7.5		200.0 ±2.5	198.8 ±0.9					
	2	199.5 ±1.9	200.0 ±2.5		198.0 ±1.5			17.6 ±0.2		
	3	198.7 ±0.8	198.8 ±0.9	198.0 ±1.5					17.7 ±0.2	
J = 5→6	0	17.7 ±0.2						198.5 ±1.3	198.7 ±0.6	198.3 ±0.3
	1									
	2			17.6 ±0.2		198.5 ±1.3			198.8 ±1.0	198.3 ±0.4
	3				17.7 ±0.2	198.7 ±0.6		198.8 ±1.0		197.9 ±0.7
	4					198.3 ±0.3		198.3 ±0.4	197.9 ±0.7	

Figure 4. Distortion Constants of $C^{12}H_3Cl^{35}$. The calculations are based on data reported by Thomas, Cox, and Gordy (16). The constant D_{JK} appears in the large blocks along the diagonal, and the constant D_{JJ} appears in the off-diagonal blocks. Each constant was computed from the two transitions which designate its row and column.

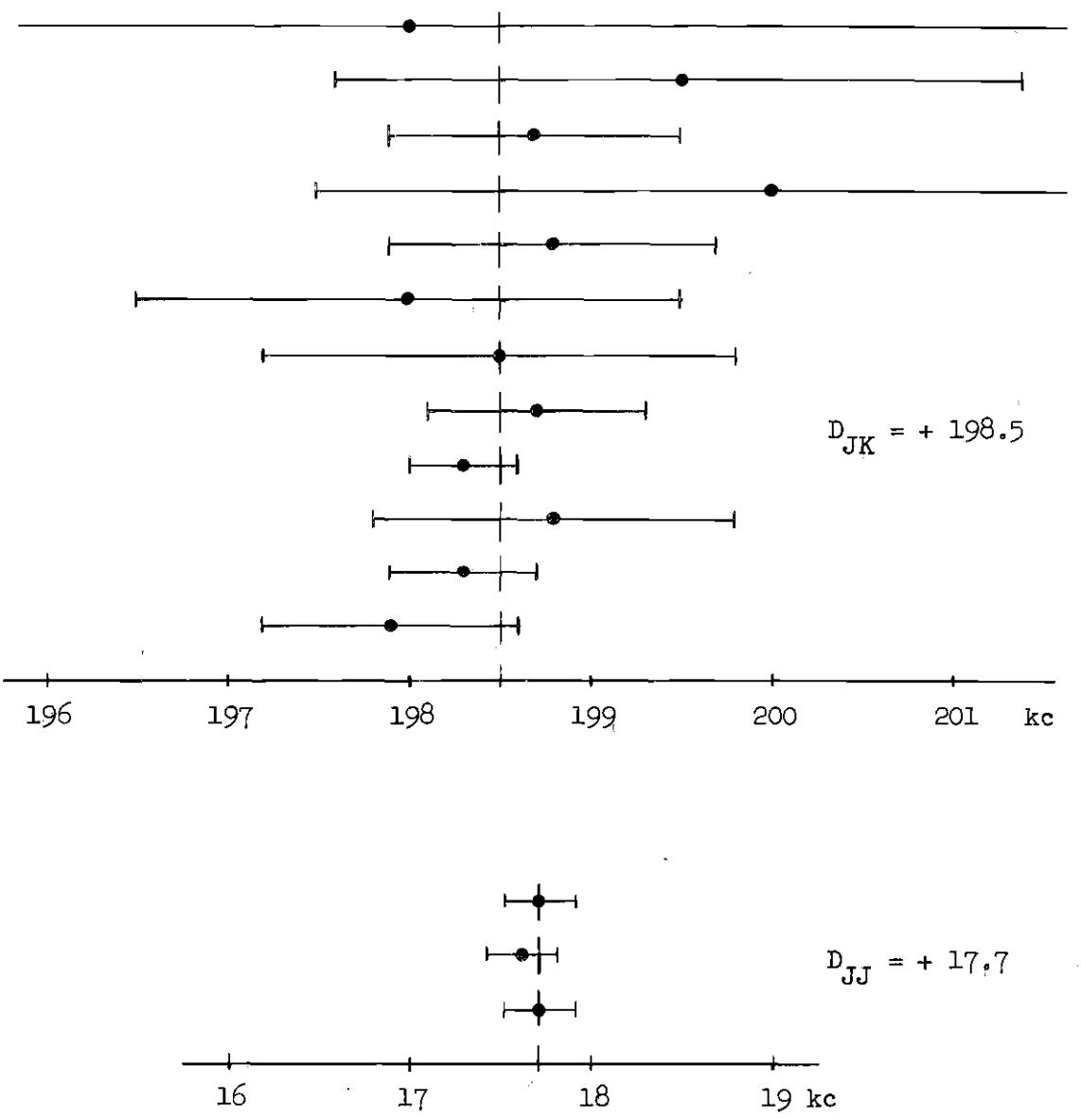

Figure 5. Weighted Distortion Constants of $C^{12}H_3Cl^{35}$. The calculations are based on data reported by Thomas,[3] Cox, and Gordy (16). The dotted lines indicate the weighted averages, and the horizontal lines indicate the estimated error of the individual calculations.

The hyperfine lines for the J = 1→2 transition were measured (see Figure 11 and Table 1), and the data were used to make additional calculations of distortion constants. The appropriate blocks in Figure 6 illustrate that the results were inconsistent; and, in fact, a negative D_{JJ} was calculated using the J = 1→2, K = 1 and the J = 2→3, K = 1 transitions. An attempt was made to measure the hyperfine lines for the J = 0→1 transition; however, the lines were not completely resolved from their Stark components (see Figure 10).

In a further effort to clear up the inconsistencies in the distortion calculations, the hyperfine lines for the J = 4→5 transition were measured (see Figure 14 and Table 1). The data were used to make additional calculations of distortion constants which are illustrated in the appropriate blocks in Figure 6. The results were still inconsistent and showed no particular trend.

An arbitrary estimated error for the unsplit lines of ±0.02 mc (based on numerous measurements, this estimated error seems to be realistic) was selected, and weighted values of the distortion constants were calculated. The results are illustrated in Figure 7. Referring to Figures 6 and 7, it can be seen that the calculated values for distortion constants are consistent for all calculations except those involving the J = 2→3 transition, which was reported by Coles and Hughes (17). This suggested that a remeasurement should be undertaken to check their data.

The hyperfine lines for the J = 2→3 and J = 3→4 transitions (see Figures 12 and 13) were measured and compared with those reported by Coles and Hughes (see Table 1). Good agreement was found for the 3→4 transition; however, slight differences were found for the 2→3 transition. Some of the weaker lines of the J = 3→4 transition, which were reported

		J = 1→2		J = 2→3		J = 3→4			J = 4→5			
	K	0	1	1	2	1	2	3	1	2	3	4
J = 1→2	0		+4.3 ±10									
	1	+4.3 ±10		-2.4 ±0.8		+0.8 ±0.3			+0.6 ±0.2			
J = 2→3	1		-2.4 ±0.8		+4.5 ±2.2	+3.1 ±0.4			+1.6 ±0.2			
	2			+4.5 ±2.2			+2.4 ±0.4			+1.4 ±0.2		
J = 3→4	1		+0.8 ±0.3	+3.1 ±0.4			+1.2 ±1.7	+1.4 ±0.6	+0.4 ±0.3			
	2				+2.4 ±0.4	+1.2 ±1.7		+1.6 ±1.0		+0.7 ±0.3		
	3					+1.4 ±0.6	+1.6 ±1.0				+0.8 ±0.3	
J = 4→5	1		+0.6 ±0.2	+1.6 ±0.2		+0.4 ±0.3				+3.1 ±1.3	+2.3 ±0.5	+2.2 ±0.3
	2				+1.4 ±0.2		+0.7 ±0.3		+3.1 ±1.3		+1.8 ±0.8	+2.0 ±0.3
	3							+0.8 ±0.3	+2.3 ±0.5	+1.8 ±0.8		+2.1 ±0.6
	4								+2.2 ±0.3	+2.0 ±0.3	+2.1 ±0.6	

Figure 6. Distortion Constants of $C^{12}Cl^{35}F_3$. The calculations are based on data for J = 2→3 and 3→4 reported by Coles and Hughes (17) and data for J = 1→2 and 4→5 measured in the present investigation. The constant D_{JK} appears in the large blocks along the diagonal, and the constant D_{JJ} appears in the off-diagonal blocks. Each constant was computed from the two transitions which designate its row and column.

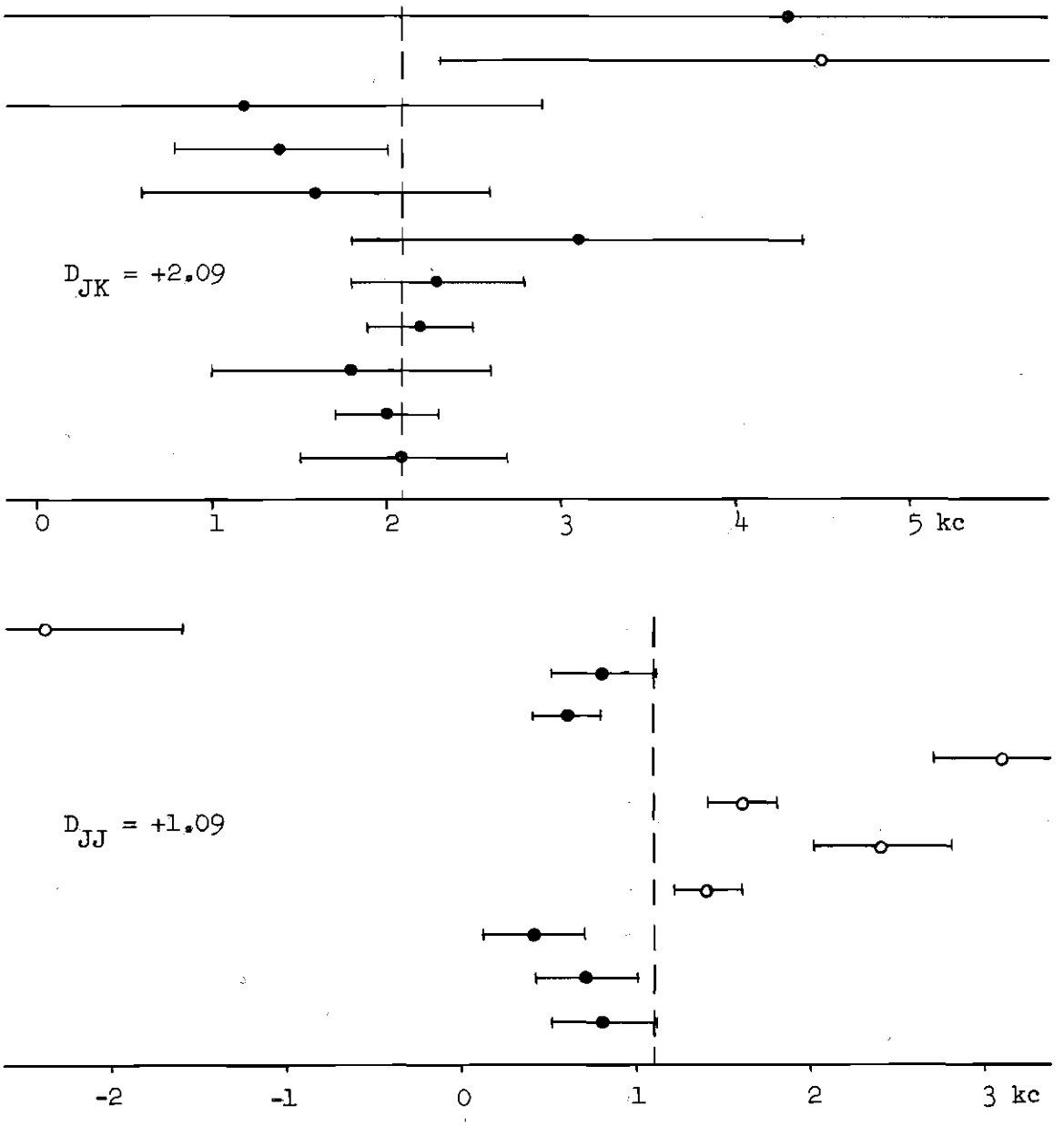

Figure 7. Weighted Distortion Constants of $C^{12}Cl^{35}F$. The calculations are based on data for J = 2→3 and 3→4 reported by Coles and Hughes (17) and data for J = 1→2 and 4→5 measured in the present investigation. The dotted lines indicate the weighted averages, and the horizontal lines indicate the estimated error of the individual calculations. Calculations involving the J = 2→3 transition are indicated by empty circles.

		J = 1→2		J = 2→3		J = 3→4			J = 4→5			
	K	0	1	1	2	1	2	3	1	2	3	4
J = 1→2	0		5.5 ±10									
	1	5.5 ±10		1.2 ±0.8		0.8 ±0.3			0.6 ±0.2			
J = 2→3	1		1.2 ±0.8		1.1 ±2.2	0.5 ±0.4			0.4 ±0.2			
	2			1.1 ±2.2			0.6 ±0.4			0.6 ±0.2		
J = 3→4	1		0.8 ±0.3	0.5 ±0.4			1.7 ±1.7	1.7 ±0.6	0.4 ±0.3			
	2				0.6 ±0.4	1.7 ±1.7		1.7 ±1.0		0.6 ±0.3		
	3					1.7 ±0.6	1.7 ±1.0				0.6 ±0.3	
J = 4→5	1		0.6 ±0.2	0.4 ±0.2		0.4 ±0.3				3.1 ±1.3	2.3 ±0.5	2.2 ±0.3
	2				0.6 ±0.2		0.6 ±0.3		3.1 ±1.3		1.8 ±0.8	2.0 ±0.3
	3							0.6 ±0.3	2.3 ±0.5	1.8 ±0.8		2.1 ±0.6
	4								2.2 ±0.3	2.0 ±0.3	2.1 ±0.6	

Figure 8. Distortion Constants of $C^{12}Cl^{35}F_3$. The calculations are based on present data from Table 1. The constant D_{JK} appears in the large blocks along the diagonal, and the constant D_{JJ} appears in the off-diagonal blocks. Each constant was computed from the two transitions which designate its row and column.

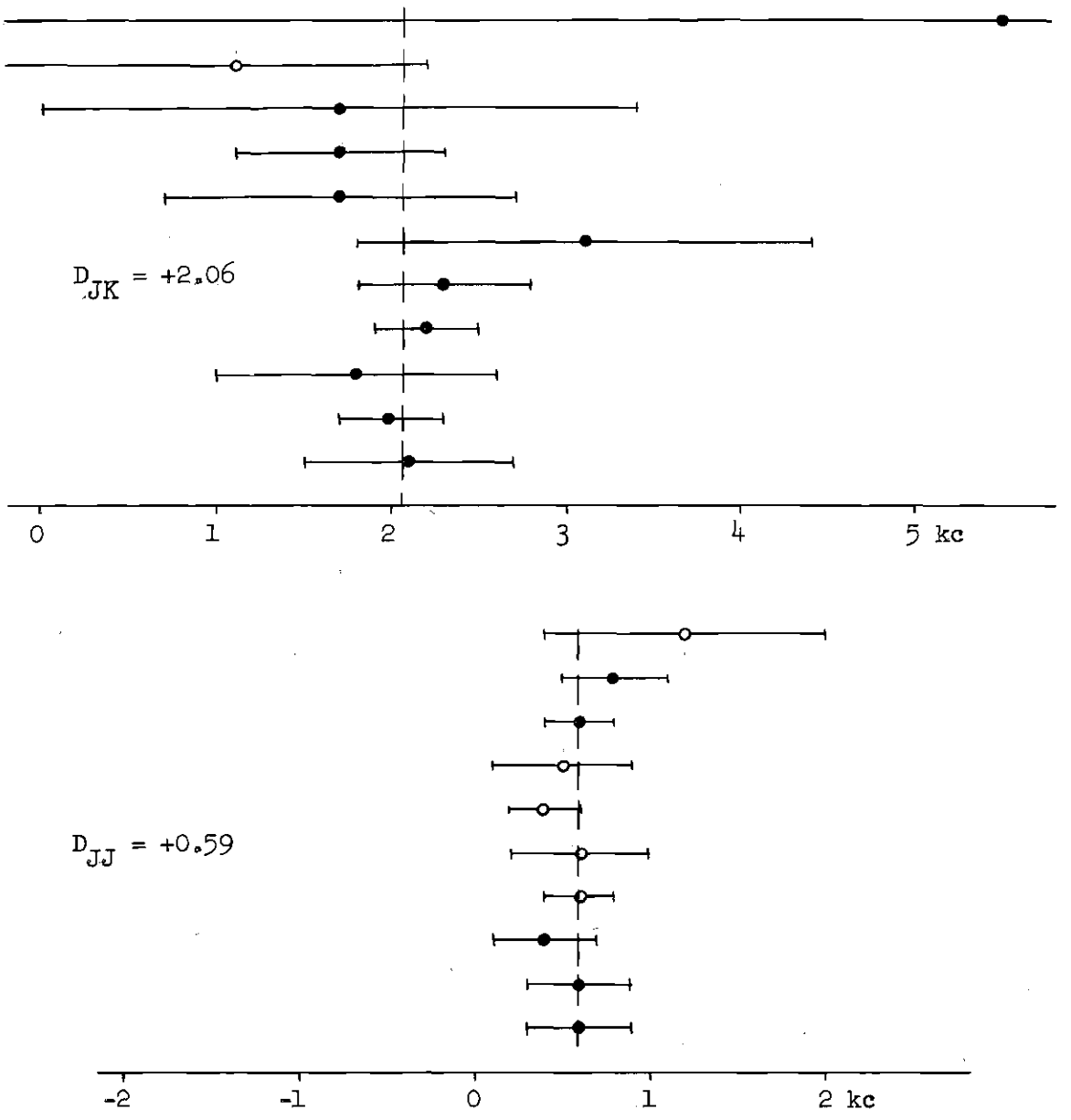

Figure 9. Weighted Distortion Constants of $C^{12}Cl^{35}F_3$. The calculations are based on present data from Table 1. The dotted lines indicate the weighted averages, and the horizontal lines indicate the estimated error of the individual calculations. Calculations involving the J = 2→3 transition are indicated by empty circles.

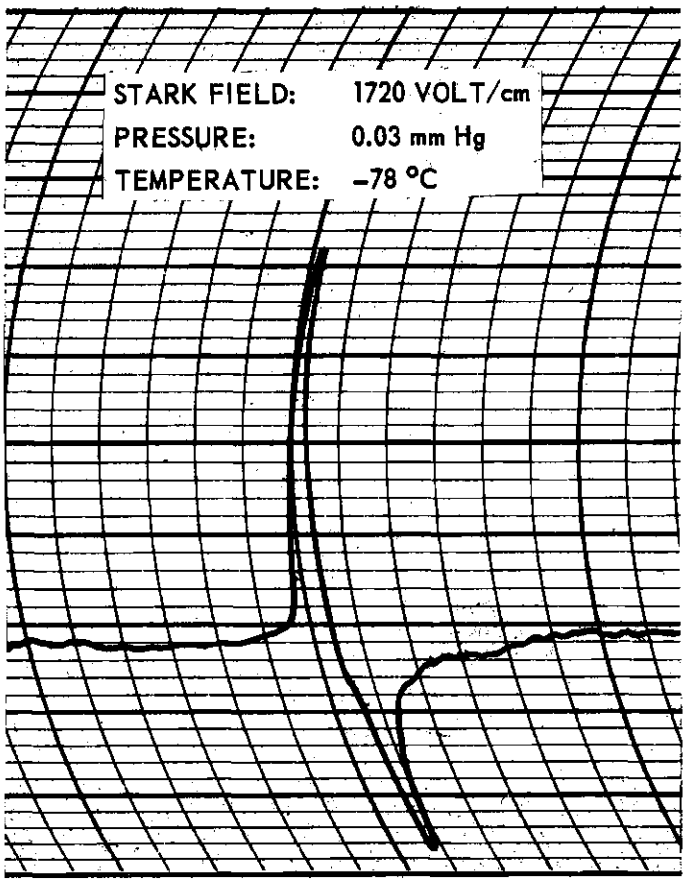

Figure 10. Recording of the J = 0→1 Transition of $C^{12}Cl^{35}F_3$.

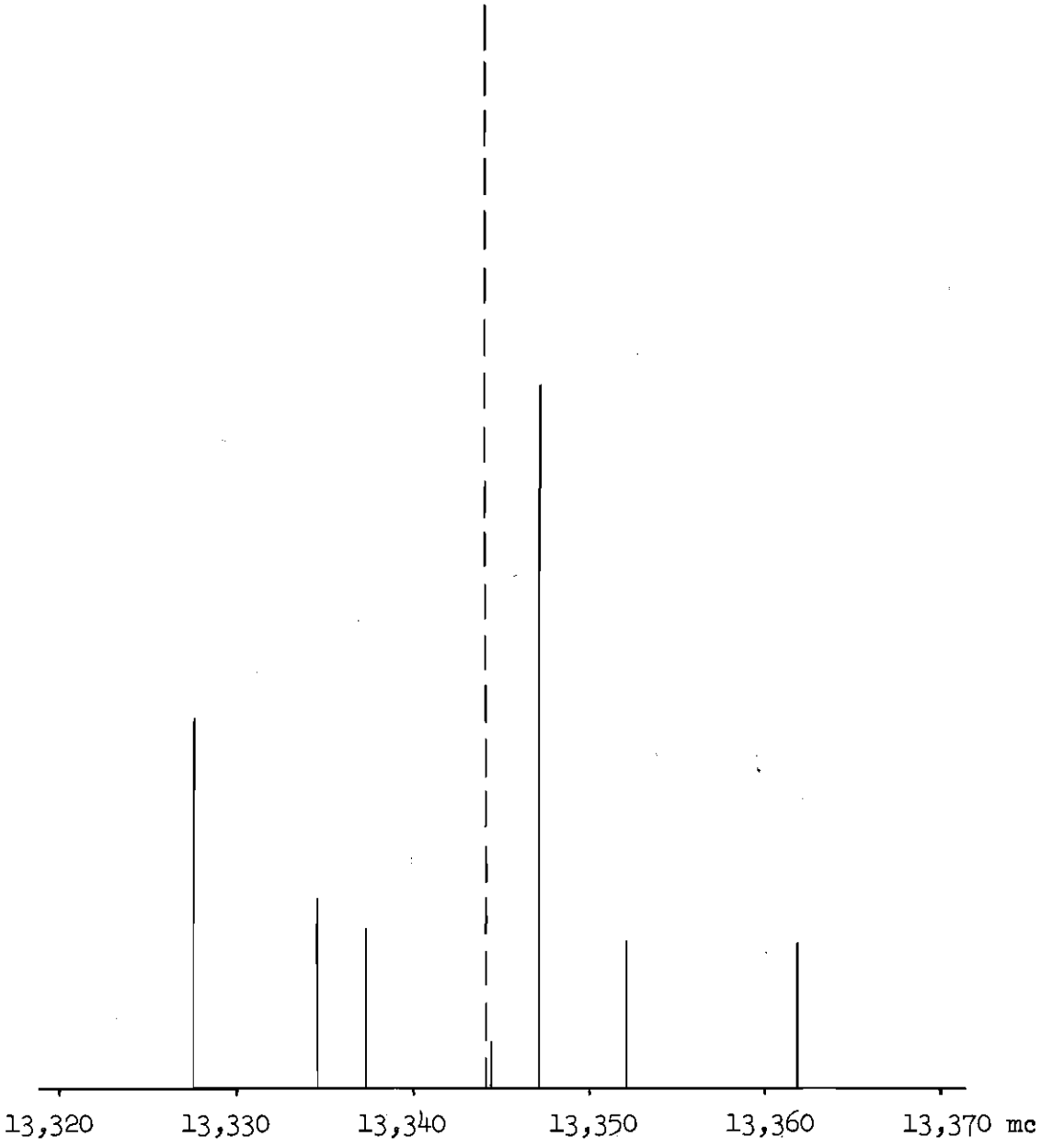

Figure 11. Theoretical Hyperfine Structure of the $J = 1 \rightarrow 2$ Transition of $C^{12}Cl^{35}F_3$. The major $K = 0$ line is shown dashed.

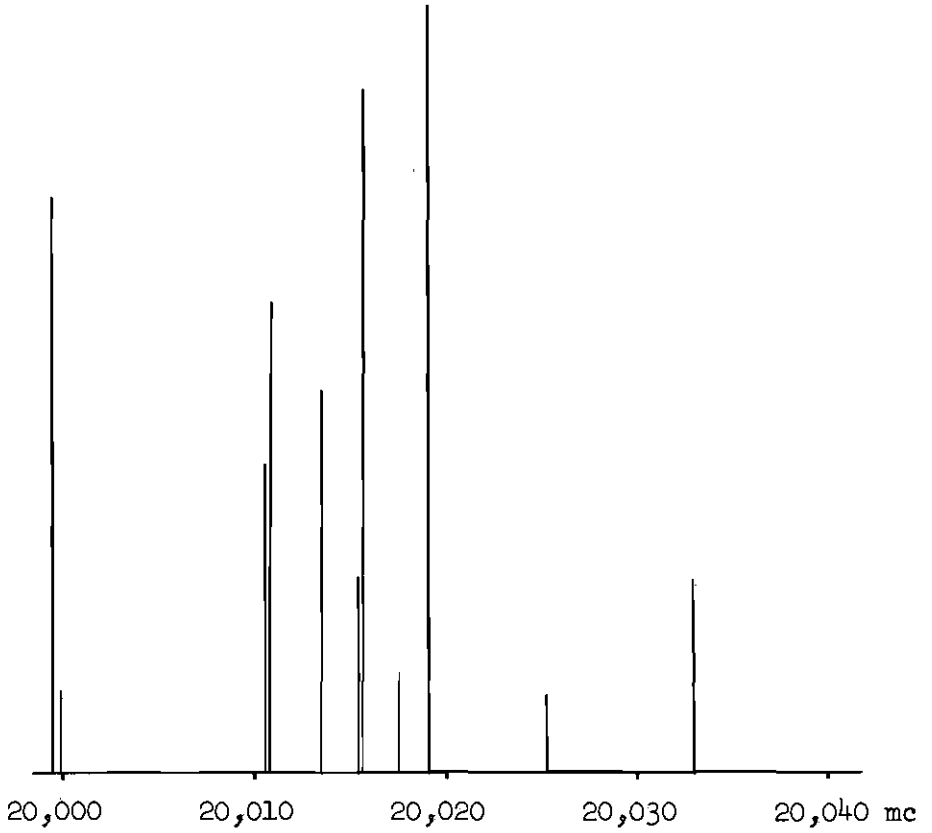

Figure 12. Theoretical Hyperfine Structure (Neglecting K = 0 Lines) of the J = 2→3 Transition of $C^{12}Cl^{35}F_3$.

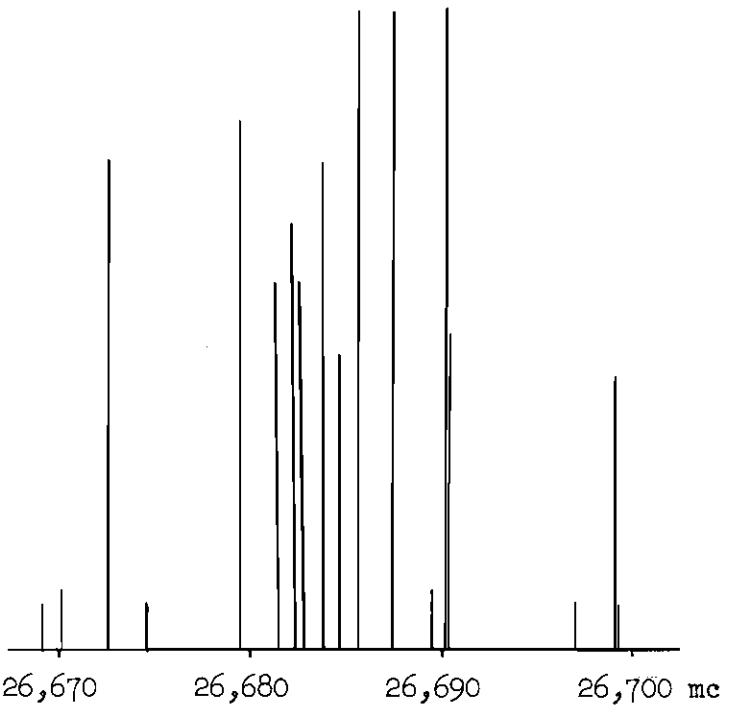

Figure 13. Theoretical Hyperfine Structure (Neglecting K = 0 Lines) of the J = 3→4 Transition of $C^{12}Cl^{35}F_3$.

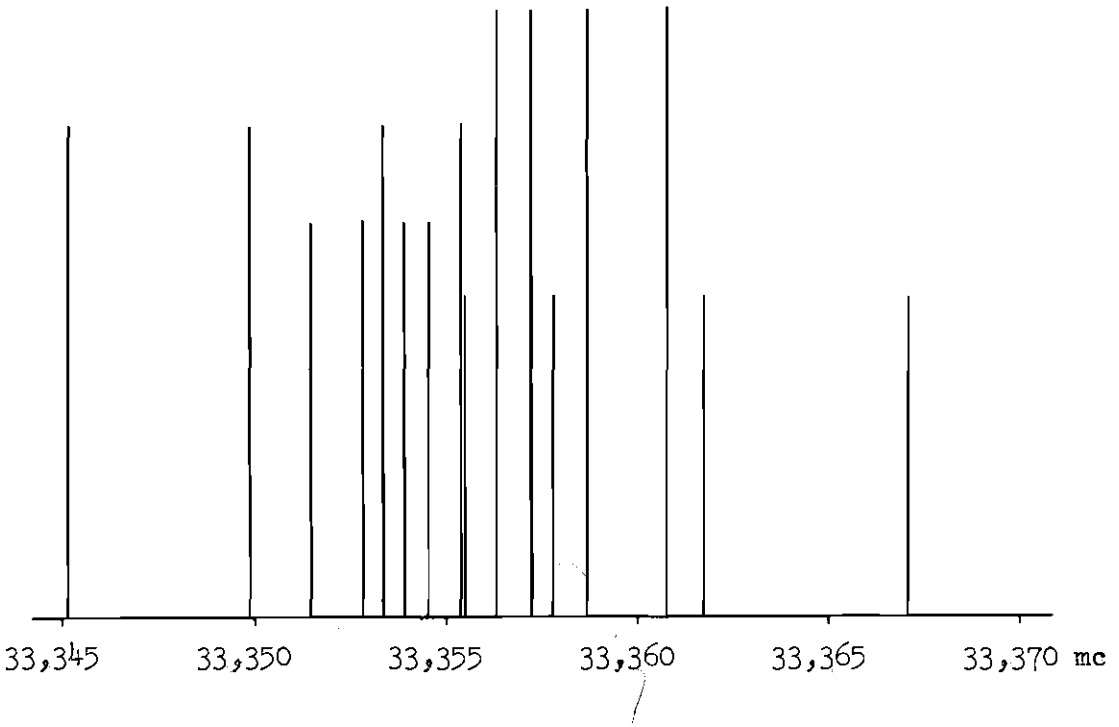

Figure 14. Major Components of the Theoretical Hyperfine Structure (Neglecting K = 0 Lines) of the J = 4→5 Transition of $C^{12}Cl^{35}F_3$.

Table 1. Measured Hyperfine Line Frequencies for $C^{12}Cl^{35}F_3$.[a]

J	K	F	Theoretical[b]	Measured Present	Measured Coles and Hughes (17)
1→2	0	3/2→5/2	13,344.03	13,344.06	
		5/2→7/2			
	1	3/2→5/2	13,327.59	13,327.59	
		5/2→7/2	13,347.09	13,347.11	
2→3	1	1/2→3/2	20,015.46	20,015.53[c]	20,015.77[c]
		3/2→5/2	20,010.59	20,010.65[c]	20,010.84[c]
		5/2→7/2	20,010.73	20,010.65[c]	20,010.84[c]
		7/2→9/2	20,015.59	20,015.53[c]	20,015.77[c]
	2	3/2→5/2	20,013.47	20,013.39	20,013.68
		3/2→3/2			
		5/2→7/2	19,999.55	19,999.57	19,999.66
		5/2→5/2			
		5/2→3/2			
		7/2→9/2	20,019.04	20,019.04	20,019.17
		7/2→7/2			
		7/2→5/2			
3→4	1	3/2→5/2	26,684.74	26,684.72	26,684.69
		5/2→7/2	26,682.79		26,682.81
		7/2→9/2	26,683.80	26,683.80	26,683.78
		9/2→11/2	26,685.75	26,685.73	26,685.73

(Continued)

Table 1. Measured Hyperfine Line Frequencies for $C^{12}Cl^{35}F_3$ (Continued).

J	K	F	Theoretical[b]	Measured Present	Measured Coles and Hughes (17)
3→4	2	3/2→5/2 5/2→5/2	26,690.12	26,690.12[c]	26,690.14[c]
		5/2→7/2 7/2→7/2	26,682.32		26,682.30
		7/2→9/2 9/2→9/2	26,679.59	26,679.58	26,679.62
		9/2→11/2	26,687.39	26,687.38	26,687.38
	3	3/2→5/2	26,699.09	26,699.10	26,699.14
		5/2→7/2	26,681.55	26,681.53	26,681.52
		5/2→5/2	26,674.72		26,674.77
		7/2→9/2	26,672.57	26,672.58	26,672.59
		7/2→7/2	26,670.17		26,670.19
		9/2→9/2	26,696.93		26,697.04
		9/2→11/2	26,690.11	26,690.12[c]	26,690.14[c]
4→5	1	5/2→7/2	33,355.50	33,355.42[c]	
		7/2→9/2	33,354.53	33,354.52	
		9/2→11/2	33,355.39	33,355.42[c]	
		11/2→13/2	33,356.36	33,356.40	

(Continued)

Table 1. Measured Hyperfine Line Frequencies for $C^{12}Cl^{35}F_3$ (Continued).

J	K	F	Theoretical[b]	Measured Present	Measured Coles and Hughes (17)
4→5	2	5/2→7/2	33,357.81	33,357.80	
		7/2→9/2	33,353.91	33,353.90	
		9/2→11/2	33,353.34	33,353.28	
		11/2→13/2	33,357.24	33,357.27	
	3	5/2→7/2	33,361.64	33,361.60	
		7/2→9/2	33,352.87	33,352.95	
		9/2→11/2	33,349.93	33,349.91	
		11/2→13/2	33,358.70	33,358.71	
	4	5/2→7/2	33,367.03	33,367.04	
		7/2→9/2	33,351.43	33,351.47	
		9/2→11/2	33,345.16	33,345.17	
		11/2→13/2	33,360.76	33,360.72	

[a] Line frequencies are in megacycles per second.

[b] Theoretical line frequencies were calculated from the constants B = 3335.596 mc, eqQ = -77.98 mc, D_{JJ} = +0.59 kc, and D_{JK} = +2.06 kc, which were evaluated from the present data.

[c] Unresolved lines.

by Coles and Hughes (17), were not remeasured because of the good agreement found for the other lines of this transition. The calculations for the distortion constants using measurements made by this author are illustrated in Figures 8 and 9. It should be noted that all calculations are now consistent; for this reason, the J = 2→3 data reported by Coles and Hughes (17) is believed to be slightly in error. If this is the case, then $C^{12}Cl^{35}F_3$ obeys Equation 27 within the limits of experimental errors.

Using present data from Table 1, the following constants were calculated:

$$B = 3335.596 \text{ mc}$$
$$eqQ = -77.98 \text{ mc}$$
$$D_{JJ} = +0.59 \text{ kc}$$
$$D_{JK} = +2.06 \text{ kc} \quad .$$

Values reported by Coles and Hughes (17) are

$$B = 3335.56 \text{ mc}$$
$$eqQ = -78.05 \text{ mc} \quad .$$

Trifluoromethane, CHF_3

The microwave absorption spectrum of trifluoromethane has been analyzed and reported by Burrus and Gordy (15). It should be noted that the atoms in this molecule have no quadrupole moment; therefore, no hyperfine splitting occurs. The center of mass for this molecule is well within the YZ_3 tetrahedron and D_{JK} turns out to be negative as expected. The resolved lines, reported in Reference 15, for the J = 3→4, J = 6→7, and J = 8→9 transitions were used in all possible combinations to calculate distortion constants.

In order to extend the investigation lower in J-values, the $J = 0 \rightarrow 1$ transition was measured by this author and found to occur at

$$20{,}697.72 \text{ mc} \quad .$$

This datum was used in conjunction with data on the other transitions to calculate additional values for the distortion constant D_{JJ}. The complete results are illustrated in Figure 15. The estimated errors were obtained by assigning ± 0.03 mc to the $J = 0 \rightarrow 1$ transition and using other estimated errors as reported in Reference 15. All evaluations of the distortion constants are consistent within the limits of experimental errors.

The weighted values of distortion constants for $C^{12}HF_3$ were found to be

$$D_{JJ} = + 11.37 \text{ kc}$$

and

$$D_{JK} = - 18.05 \text{ kc} \quad ,$$

as illustrated in Figure 16. These compare well with the values reported by Burrus and Gordy (15),

$$D_{JJ} = + 11.3 \text{ kc}$$

and

$$D_{JK} = - 18.0 \text{ kc} \quad .$$

For Figure 16, the estimated errors of the line frequencies reported by Burrus and Gordy have been reduced by a factor of ten, and consistent results were still obtained. This seems to indicate that their assignment of estimated errors may be too generous.

		J = 0→1	J = 3→4		J = 6→7							J = 8→9								
	K	0	2	3	0	1	2	3	4	5	6	0	1	2	3	4	5	6	7	8
J = 0→1	0				+11.5 ±0.3							+11.5 ±0.2								
J = 3→4	2			-17.2 ±10.0			+11.3 ±0.7							+11.3 ±0.4						
	3		-17.2 ±10.0					+11.3 ±0.7							+11.3 ±0.4					
J = 6→7	0	+11.5 ±0.3				-17.8 ±42.0	-18.0 ±10.5	-17.9 ±4.7	-18.0 ±2.6	-18.1 ±1.7	-18.1 ±1.2	+11.4 ±0.7								
	1				-17.8 ±42.0		-18.1 ±14.0	-18.0 ±5.3	-18.0 ±2.8	-18.1 ±1.8	-18.1 ±1.2		+11.3 ±0.7							
	2		+11.3 ±0.7		-18.0 ±10.5	-18.1 ±14.0		-17.9 ±8.4	-18.0 ±3.5	-18.1 ±2.0	-18.1 ±1.3			+11.4 ±0.7						
	3			+11.3 ±0.7	-17.9 ±4.7	-18.0 ±5.3	-17.9 ±8.4		-18.1 ±6.0	-18.1 ±2.6	-18.2 ±1.6				+11.4 ±0.7					
	4				-18.0 ±2.6	-18.0 ±2.8	-18.0 ±3.5	-18.1 ±6.0		-18.2 ±4.7	-18.2 ±2.1					+11.4 ±0.7				
	5				-18.1 ±1.7	-18.1 ±1.8	-18.1 ±2.0	-18.1 ±2.6	-18.2 ±4.7		-18.3 ±3.8						+11.3 ±0.7			
	6				-18.1 ±1.2	-18.1 ±1.2	-18.1 ±1.3	-18.2 ±1.6	-18.2 ±2.1	-18.3 ±3.8								+11.4 ±0.7		
J = 8→9	0	+11.5 ±0.2			+11.4 ±0.7								-20.5 ±44.0	-18.2 ±11.0	-18.0 ±4.9	-18.1 ±2.8	-18.1 ±1.8	-18.1 ±1.2	-18.1 ±0.9	-18.1 ±0.7
	1					+11.3 ±0.7						-20.5 ±44.0		-17.4 ±14.7	-17.7 ±5.5	-17.9 ±2.9	-18.0 ±1.8	-18.0 ±1.3	-18.0 ±0.9	-18.0 ±0.7
	2		+11.3 ±0.4				+11.4 ±0.7					-18.2 ±11.0	-17.4 ±14.7		-17.9 ±8.8	-18.0 ±3.7	-18.1 ±2.1	-18.1 ±1.4	-18.1 ±1.0	-18.1 ±0.7
	3			+11.3 ±0.4				+11.4 ±0.7				-18.0 ±4.9	-17.7 ±5.5	-17.9 ±8.8		-18.1 ±6.3	-18.2 ±2.8	-18.1 ±1.6	-18.1 ±1.1	-18.1 ±0.8
	4								+11.4 ±0.7			-18.1 ±2.8	-17.9 ±2.9	-18.0 ±3.7	-18.1 ±6.3		-18.2 ±4.9	-18.1 ±2.2	-18.1 ±1.3	-18.1 ±0.9
	5									+11.3 ±0.7		-18.1 ±1.8	-18.0 ±1.8	-18.1 ±2.1	-18.2 ±2.8	-18.2 ±4.9		-18.0 ±4.0	-18.0 ±1.8	-18.0 ±1.1
	6										+11.4 ±0.7	-18.1 ±1.2	-18.0 ±1.3	-18.1 ±1.4	-18.1 ±1.6	-18.1 ±2.2	-18.0 ±4.0		-18.0 ±3.4	-18.0 ±1.6
	7											-18.1 ±0.9	-18.0 ±0.9	-18.1 ±1.0	-18.1 ±1.1	-18.1 ±1.3	-18.0 ±1.8	-18.0 ±3.4		-18.0 ±2.9
	8											-18.1 ±0.7	-18.0 ±0.7	-18.1 ±0.7	-18.1 ±0.8	-18.1 ±0.9	-18.0 ±1.1	-18.0 ±1.6	-18.0 ±2.9	

Figure 15. Distortion Constants of $C^{12}HF_3$. The calculations are based on data for J = 3→4, 6→7, and 8→9 reported by Burrus and Gordy (15) and data for J = 0→1 measured in the present investigation. The constant D_{JK} appears in the large blocks along the diagonal, and the constant D_{JJ} appears in the off-diagonal blocks. Each constant was computed from the two transitions which designate its row and column.

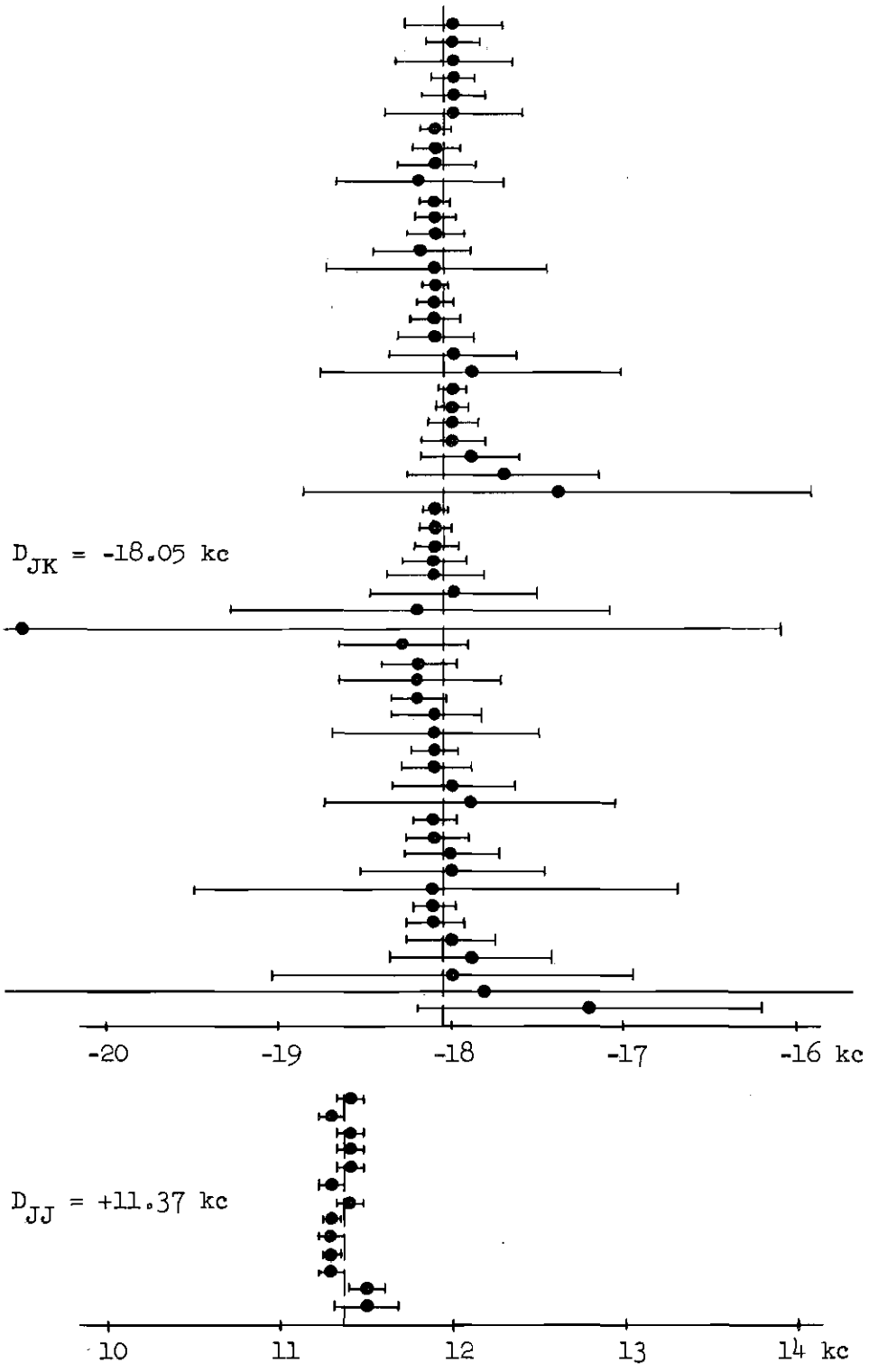

Figure 16. Weighted Distortion Constants of $C^{12}HF_3$. The estimated errors for the lines reported by Burrus and Gordy (15) have been reduced by a factor of ten.

Higher-Order Distortion Constants and CCl_3F

In the recent investigation (3) of CCl_3F, the J = 1→2 and 2→3 transitions were analyzed in detail, and measurements were made for the frequencies of the largest resolvable prominence for each of the rotational transitions J = 3→4 through 6→7. The frequency shift of the most intense hyperfine component for any J→J+1 transition belongs to the set K = 1 and is specified by F = (J+7/2)→(J+9/2). The expression for the frequency shift (32) is

$$\nu_Q = \beta(J)eqQ \quad ,$$

where

$$\beta(J) = -\frac{3}{4}\frac{(J+1)(J+2) + (4J+7)}{(2J+5)(2J+3)(J+2)(J+1)}$$

and q is the second partial derivative of the electric potential at the chlorine nucleus (resulting from extranuclear charges) with respect to z, the symmetry axis of the molecule. Results of the measurements are given in Table 2.

The increasing value of $(\nu-\nu_Q)/2(J+1)$ with increasing J in Table 2 is a strange effect, if one assumes that it is the result of centrifugal stretching, because it implies a negative value of D_{JJ}. Calculations (3) based on the J = 1→2 data and the J = 2→3 through 6→7 data yield for D_{JJ} the values: - 24 ± 2 kc and - 14 kc, - 9 kc, - 6 kc, and - 4 kc with probable errors less than ± 1 kc. The observed variation of D_{JJ} with J suggests a possible need for considering higher-order distortion constants.

Table 2. Frequencies of the Strongest Line (K=1) in Various Transitions for $C^{12}Cl_3^{35}F$.[a]

Transition J→J+1	Measured Frequency, ν, of Strongest Line (mc)	ν_Q [b]	$\frac{\nu-\nu_Q}{2(J+1)}$
1→2	9 859.30 ± 0.04	- 2.26 ± 0.03	2465.39 ± 0.01
2→3	14 792.80 ± 0.06	- 1.00 ± 0.01	2465.63 ± 0.01
3→4	19 725.17 ± 0.01	- 0.55 ± 0.01	2465.72 ± 0.00
4→5	24 657.26 ± 0.03	- 0.35 ± 0.00	2465.76 ± 0.00
5→6	29 588.95 ± 0.01	- 0.23 ± 0.00	2465.76 ± 0.00
6→7	34 520.42 ± 0.01	- 0.17 ± 0.00	2465.76 ± 0.00

[a] From Reference 3.

[b] eqQ = 37.3 ± 0.5 mc based on J = 1→2 data.

If the third-order terms of a Taylor's expansion of the energy are retained, the equivalent of Equation 27 for a transition J→J+1 and $\Delta K = 0$ becomes

$$\frac{\nu'}{2(J+1)} = B - 2(J+1)^2 D_{JJ} - K^2 D_{JK} - (J+1)^2(3J^2+6J+4)D_{JJJ} - 2(J+1)^2K^2 D_{JJK} - K^4 D_{JKK} \quad , \tag{28}$$

where $\nu' = \nu - \nu_Q$ is the unsplit line frequency and D_{JJJ}, D_{JJK}, and D_{JKK} are defined as second-order distortion constants (see Appendix A). An effort was made to fit the CCl_3F data to Equation 28, and the data was found to be inconsistent.

In Appendix A, it is shown that any nonrigid symmetric-top molecule should obey Equation 28, or a similar equation including additional higher

order terms. However, it seems highly unlikely that the energy expression, as a function of J and K, has a higher-order "wrinkle" for low J-values. It is more conceivable that higher-order distortion constants are required for high J transitions; this fact has been observed by Cowan and Gordy (33) while investigating $Br^{81}CN$ for transitions involving J = 47→48, J = 51→52, and J = 55→56.

The fact that the CCl_3F data cannot be described by Equation 28 seems to indicate that the unsplit line frequencies of Table 2 are incorrect. If so, this would indicate either (a) an error in determining the frequencies of the strongest hyperfine lines or (b) an error in the calculated quadrupole frequency shift. Both of these possibilities have been discussed by Long (34); however, no suitable explanation could be found. It is interesting to note that, if eqQ is arbitrarily increased by a factor of 5/3, the unsplit line frequencies are well behaved and indicate a rotational constant D_{JJ} approximately equal to zero. However, this is unsatisfactory because the quadrupole coupling constant, assuming extranuclear charge symmetry about the C-Cl bond, is already large compared to values obtained for other molecules.

Theoretical Rotational Distortion Constants

A theoretical approach for calculating distortion constants was undertaken by Slawsky and Dennison (1). They applied the theory of the semi-rigid rotor, which was developed by Wilson and Howard (18), to the symmetric molecules YZ_3 and XYZ_3. It was found that the change in rotational energy, caused by centrifugal distortions, can be expressed in terms of the quantum numbers J and K and as a function of the potential constants and the molecular dimensions. The numerical calculations,

however, are rather involved and laborious. Agreement between theoretical values, based on calculations of this type, and experimental values for distortion constants were fair for most molecules considered.

More recently, the calculation of rotational distortion constants for some axially symmetric XYZ_3 molecules was considered by Dowling, Gold, and Meister (5, 6). Explicit equations were written for the rotational distortion constants D_{JJ}, D_{JK}, and D_{KK} in terms of the nuclear masses, bond lengths, bond angles, and the molecular force constants.

For axially symmetric molecules of the XYZ_3 type, the principal symmetry axis passes through the X and Y atoms as illustrated in Figure 17. Molecules of this type are said to belong to the C_{3v} point group (19, 20); the subscript 3v means that there are three vertical planes of symmetry and that the covering operations consist of three reflections and three rotations.

The rotational distortion constants of a molecule belonging to the C_{3v} point group can be written (5) in the form

$$D_{JJ} = \frac{\epsilon t_{xxxx}}{8(I^o_{xx})^4} \quad , \tag{29}$$

$$D_{JK} = -2D_{JJ} + \frac{\epsilon(t_{xxzz} + 2t_{xzxz})}{4(I^o_{xx})^2(I^o_{zz})^2} \quad , \tag{30}$$

and

$$D_{KK} = -D_{JJ} - D_{JK} + \frac{\epsilon t_{zzzz}}{8(I^o_{zz})^4} \quad , \tag{31}$$

where $I^o_{\alpha\alpha}$ is the $\alpha\alpha$-component of the moment of inertia tensor evaluated

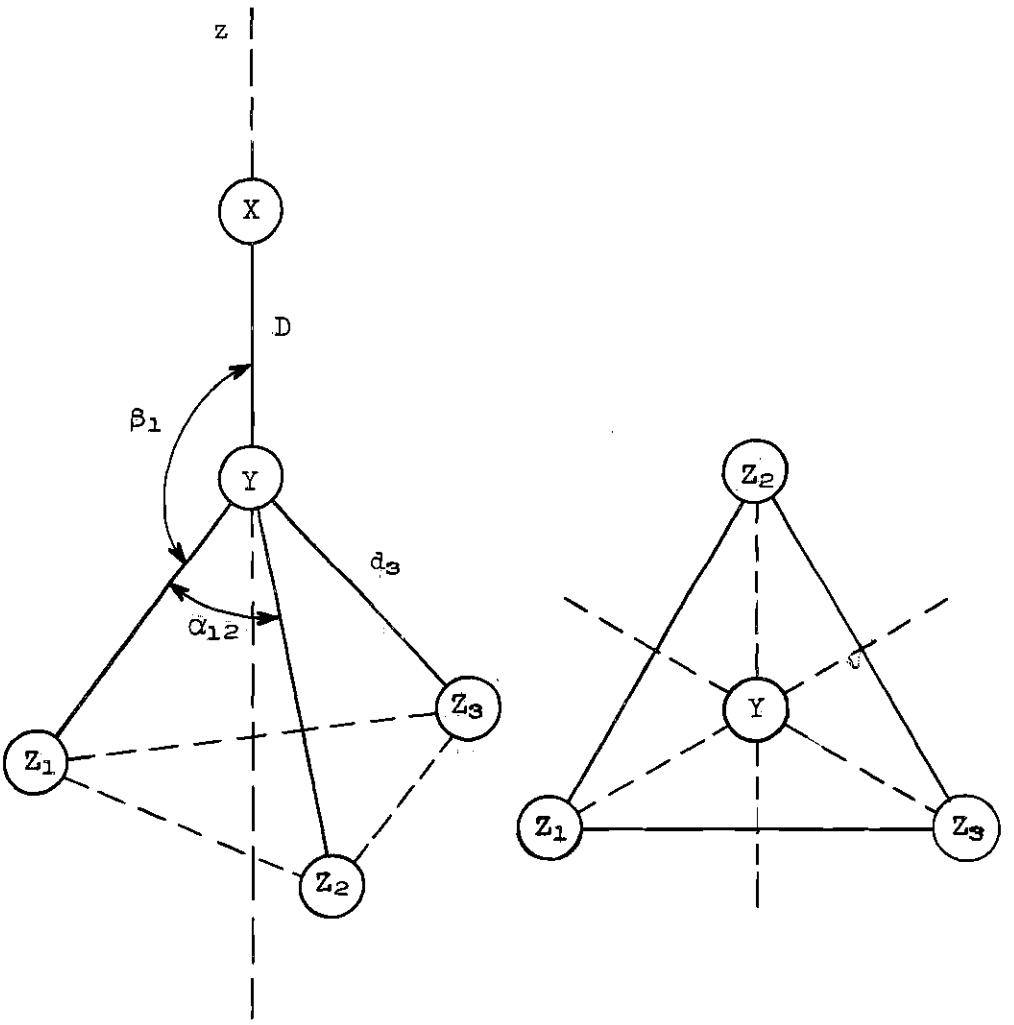

(a) Side View (b) End View

Figure 17. An XYZ_3 Molecule Belonging to the $^3C_{3v}$ Group.

at equilibrium for a molecule in its center of mass, principal axis system. The $t_{\alpha\beta\gamma\delta}$'s may be written as

$$t_{\alpha\beta\gamma\delta} = \sum_{ik} \left[J^i_{\alpha\beta}\right]_o (F^{-1})_{ik} \left[J^k_{\gamma\delta}\right]_o \quad , \tag{32}$$

where $\left[J^i_{\alpha\beta}\right]_o$ is the partial derivative (evaluated at equilibrium) of the $\alpha\beta$-component of the moment of inertia tensor with respect to the i^{th} symmetry coordinate and $(F^{-1})_{ik}$ is an element of the matrix inverse to the potential energy matrix written in terms of the symmetry coordinates. The $\left[J^i_{\alpha\beta}\right]_o$ are given in Table 6 of Appendix E. In general, the F matrix will be factored in blocks along the diagonal and therefore so will the F^{-1} matrix. For an XYZ_3 molecule of C_{3v} symmetry, F^{-1} will consist of three 3×3 matrices, two of which will be identical. The constant ϵ multiplying each $t_{\alpha\beta\gamma\delta}$ is 6.7731×10^5 kc/sec, if the masses are in atomic mass units, the internuclear distances are in Angstroms, the F matrix elements corresponding to the stretching bonds and the interaction between the stretching of bonds are in millidyne/Angstrom, the F matrix elements corresponding to the interaction between bending and stretching are in millidyne/radian, and the F matrix elements corresponding to bending and the interaction between bending and bending are in millidyne Angstrom/radian^2.

If one assumes harmonic motion of small amplitude for the nuclei, the expression for the potential energy V of the molecule can be written (21) in the form

$$2V = \sum_{ij} f_{ij}\, r_i\, r_j \quad , \tag{33}$$

where $f_{ij} = f_{ji}$ are force constants related to the internal coordinates r_i and r_j. But the potential energy can also be expressed in terms of the symmetry coordinates by means of the equation

$$2V = \sum_{ij} F_{ij} R_i R_j \quad , \tag{34}$$

where F_{ij} are force constants related to the symmetry coordinates R_i and R_j. In matrix notation, these equations are

$$2V = \underline{r}' \underline{f} \underline{r} \tag{35}$$

and

$$2V = \underline{R}' \underline{F} \underline{R} \quad , \tag{36}$$

where $\underline{r}'$ and $\underline{R}'$ are the transposes of the $\underline{r}$ and $\underline{R}$ matrices. The r_i and R_i coordinates transform as

$$\underline{R} = \underline{U} \underline{r} \tag{37}$$

or

$$\underline{r} = \underline{U}' \underline{R} \tag{38}$$

where $\underline{U}'$ equals $\underline{U}^{-1}$, the inverse of $\underline{U}$. From the above

$$\begin{aligned} \underline{R}' \underline{F} \underline{R} &= \underline{r}' \underline{f} \underline{r} \\ &= \underline{R}' (\underline{U} \underline{f} \underline{U}') \underline{R} \quad , \end{aligned}$$

or

$$\underline{F} = \underline{U} \underline{f} \underline{U}' \tag{39}$$

The $\underline{F}$, $\underline{f}$, $\underline{U}$, and $\underline{U}'$ matrices are defined in Appendix E.

It is now possible to calculate the distortion constants if the following parameters are known: nuclear masses, bond lengths, bond

angles, and the appropriate force constants. The required parameters for several XCZ_3 molecules are given in Tables 3 and 4. The calculated and observed rotational distortion constants are given in Table 5. Agreement between calculated and observed constants is fair for all molecules except $CHCl_3$ and CCl_3F, the only ones considered having three identical nuclei of spin 3/2. The disagreement was very great in these two cases; this suggests a need for further investigations of these molecules.

Summary of Results

Because of the apparent violation of existing distortion theory by the molecules $CHCl_3$ and CCl_3F, detailed calculations of distortion constants were made for three other symmetric tops: CH_3Cl, $CClF_3$, and CHF_3. All three were found to obey existing distortion theory, within the limits of experimental errors, using first-order distortion constants. An attempt was made to fit the CCl_3F data from Reference 3 using distortion constants through second order, and the data were found to be inconsistent. In addition, the theoretical and observed distortion constants for nine symmetric tops were compared. Agreement was fair for all molecules considered except $CHCl_3$ and CCl_3F; the disagreement was very large in these two cases.

Table 3. Molecular Dimensions of Some XCZ_3 Molecules.[a]

Molecule	C-X	C-Z	Z-C-Z	X-C-Z	B_o	Reference
$CHCl_3^{35}$	1.073	1.767	110°24'	108°32'	3301.94	22
CHF_3	1.098	1.332	108°48'	110°8'	10,348.74	22
CH_3Br^{79}	1.9391	1.113	111°14'	107°39'	9568.40	23
CH_3Cl^{35}	1.7810	1.113	110°31'	108°24'	13,292.89	23
CH_3I	2.1392	1.113	111°25'	107°27'	7501.25	23
$CCl^{35}F_3$	1.740	1.328	108°	110°54'	3335.56	24,25[b]
$CCl_3^{35}F$	1.33	1.76	109°40'	109°16'	2465.39	3
CF_3Br^{79}	1.908	1.330	108°	110°54'	2098.06	25
CF_3I	2.134	1.332	108°	110°54'	1523.23	25

M_C = 12.001 M_{Cl} = 35.000

M_H = 1.008 M_{Br} = 79.000

M_F = 19.000 M_I = 127.00

[a] Bond lengths are in Angstroms, masses are in atomic mass units and rotational constants are in megacycles per second.

[b] The bond lengths were calculated in Reference 24 assuming tetrahedral angles; the bond lengths recorded here were given in Reference 25 assuming Z-C-Z = 108°, a more probable value.

Table 4. Force Constants of Some XCZ_3 Molecules.[a]

Molecule	f_x	f_z	f_{zz}	f_{xz}	f_x^z	f_x^{zz}	f_x^{xz}	f_z^z	Reference
$HCCl_3$	4.8002	3.4580	1.1621	0.92126	0.08800	0.63846[b]		0.30760	26
HCF_3	5.0323	6.2460	2.1523	0.94632	0.25305	0.26428[b]		0.87900	27
$BrCH_3$	2.8631	5.1199	0.53535	0.62871	0.05890	0.00000	0.25970	-0.00781	28
$ClCH_3$	3.40025	5.14435	0.54894	0.77495	0.08800	0.00000	0.33000	-0.00169	29
ICH_3	2.2467	5.0541	0.54775	0.57410	0.063509	-0.13676[b]		-0.0254	30
$ClCF_3$	3.4580	6.2460	2.1329	1.1408	0.70843	-0.73068[b]		0.87900	27
$FCCl_3$	4.9447	3.4580	1.1621	1.6580	0.90713	-0.13733[b]		0.30760	26
$BrCF_3$	3.0352	6.2460	2.1329	0.73841	0.71247	-0.26499[b]		0.87900	31
ICF_3	2.2890	6.2460	2.1329	0.51360	0.63250	-0.3640[b]		0.87900	31

[a] Bond stretching and bond interaction constants are in units of md/A (millidyne/Angstrom); angle-bond interaction constants are in md/rad; angle bending and angle interaction constants are in md A/rad^2.

[b] This force constant is $f_x^{zz} - f_x^{xz}$.

(Continued)

Table 4. Force Constants of Some XCZ_3 Molecules (Continued).

Molecule	f_z^{zz}	$f_z^{zz'}$	f_z^{xz}	$f_z^{xz'}$	f_{zz}^{xz}	$f_{zz}^{xz'}$	$f_{zz}^{zz'}$	$f_{xz}^{xz'}$	Reference
$HCCl_3$	0.36434	-0.27281	0.18601	-0.16400	0.028235	0.00000	0.08503	0.27305	26
HCF_3	0.41959	-0.2244	0.43933	-0.21967	0.31008	0.00000	0.52869	0.17901	27
$BrCH_3$	0.15645	-0.06855	0.06965	-0.05535	0.01000	0.00000	-0.01600	-0.01516	28
$ClCH_3$	0.18000	-0.08000	0.26000	-0.09100	0.06464	-0.00236	-0.01616	0.05789	29
ICH_3	0.22912	-0.09777	0.40936	0.18676	0.015916	0.00000	-0.017934	-0.001256	30
$ClCF_3$	0.41770	-0.22339	0.30557	-0.15278	0.060827	0.00000	0.52392	-0.022689	27
$FCCl_3$	0.36434	-0.27281	0.30940	-0.22571	0.06236	0.00000	0.08503	0.22068	26
$BrCF_3$	0.41770	-0.22339	0.24665	-0.09272	0.0500	0.00000	0.57700	-0.23225	31
ICF_3	0.41770	-0.22339	0.29545	-0.11430	0.0300	0.00000	0.6392	-0.28590	31

Table 5. Calculated and Observed Rotational Distortion Constants for Some XCZ_3 Molecules.[a]

Molecule	D_{JJ} Calculated	D_{JJ} Observed	D_{JK} Calculated	D_{JK} Observed	Observed Reference
$CHCl_3^{35}$	1.44[b]	4.12	-2.39[b]	55	32
		-1.8[c]		-201	4,3
CHF_3	11.4[b]	11.3	-18.2[b]	-18.0	15
CH_3Br^{79}	9.7[b]	9.9	103[b]	128.3	16
CH_3Cl^{35}	18.2[b]	18.1	175[b]	198	16
CH_3I	6.45	6.28	55.9	98.5	16
$CCl^{35}F_3$	0.55	0.59	2.00	2.06	Present
$CCl_3^{35}F$	0.46	-4[d]	-0.50	-196	3
CF_3Br^{79}	0.26[b]		1.22[b]	1.26	25
CF_3I	0.17[b]		0.88[b]	0.6	25

[a] In units of kc/sec.

[b] From Reference 5.

[c] Calculations using J = 1→2 and 2→3 data yield -14.5; calculations using J = 1→2 and 6→7 data yield -1.8.

[d] Calculations using the J = 1→2 data and the J = 2→3 through J = 6→7 data yield for D_{JJ} the values: -24 ±2 and -14, -9, -6, and -4 with probable errors less than ±1.

CHAPTER V

STARK EFFECT OF CHLOROTRIFLUOROMETHANE

Stark effects are changes in the spectrum of a system when the system is subjected to an electric field. The rotational spectrum of a molecule which has an electric dipole moment may be expected to be modified when the molecule is in an electric field, since the field exerts torques on the molecular dipole and thereby changes its rotational motion. A measurement and analysis of the Stark effect allows one to evaluate the molecular dipole moment.

The Stark effect of the symmetric top, chlorotrifluoromethane ($CClF_3$), is affected by the quadrupole coupling of the chlorine nucleus to the average gradient of the molecular electric field. The theory of Stark effects on symmetric-top molecules with nuclear quadrupole coupling has been developed by Low and Townes (35). They found it convenient to discuss three types of conditions: weak field, strong field, and intermediate field.

In the weak field case, the Stark energy is small compared to the quadrupole coupling energy. In this case, the rotational wave functions and the hyperfine structure are only slightly perturbed by the electric field. Expressed classically, the precession of the molecule due to the Stark field is so slow that the interaction between the nucleus and the molecule is very little disturbed. A vector diagram of the weak field case is illustrated in Figure 18. The molecular symmetry axis precesses rapidly about the rotational angular momentum vector $\vec{J}$. The nuclear

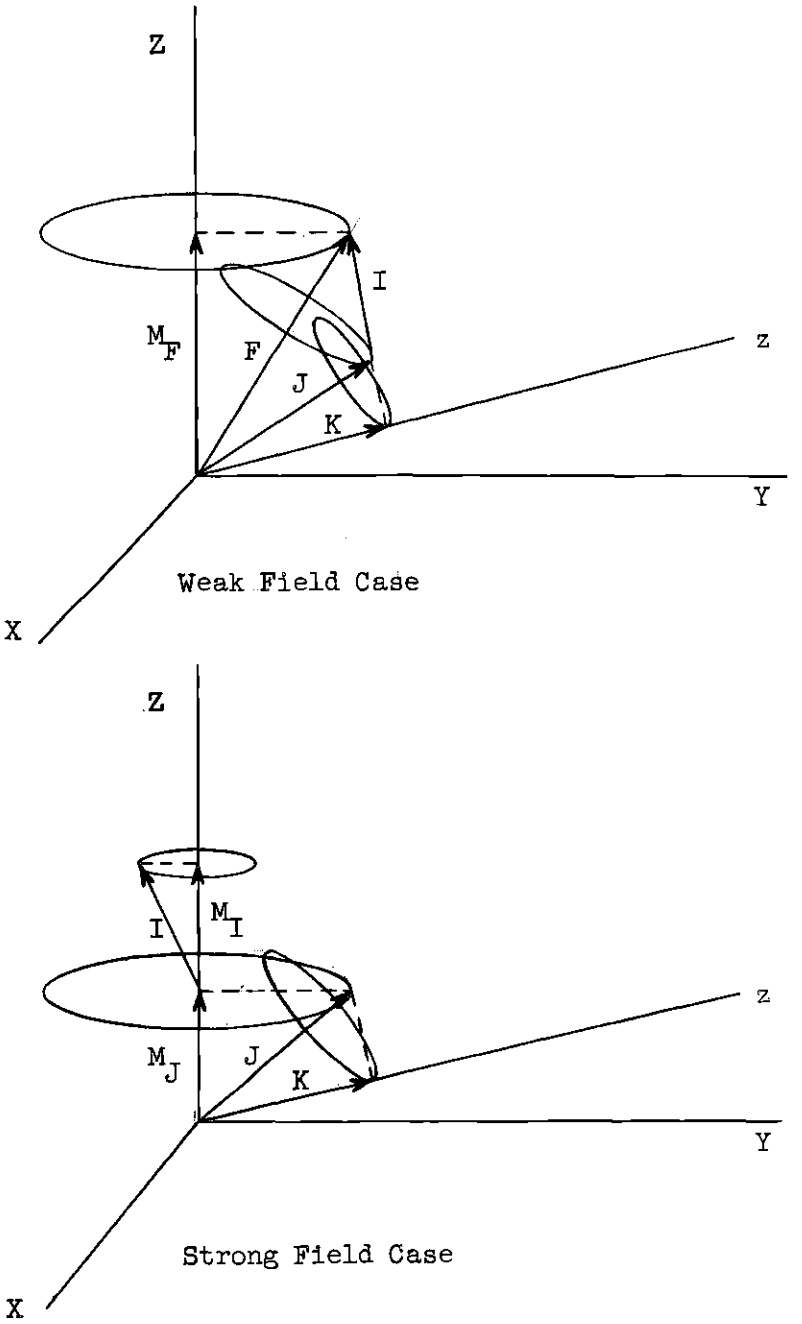

Figure 18. Vector Diagrams for the Stark Effects on Symmetric-Top Molecules With Nuclear Quadrupole Coupling.

quadrupole moment couples to the average molecular field, causing the rotational angular momentum vector $\vec{J}$ and the nuclear spin angular momentum vector $\vec{I}$ to precess slowly about the total angular momentum vector $\vec{F}$. The Stark field, oriented along the Z-axis, couples to the molecular dipole moment causing a precession, much slower than the previous two, about the Z-axis. The molecular state is satisfactorily specified by the quantum numbers, J, K, I, F, and M_F. Each hyperfine line is split by the Stark effect into various components according to the value of M_F, and this splitting is small compared with the hyperfine splitting.

In the strong field case, the Stark energy is large compared to the quadrupole coupling energy. The molecule is precessed so violently by the external field that the nuclear orientation cannot follow the motion; the vectors $\vec{J}$ and $\vec{I}$ are said to be decoupled. A vector diagram of the strong field case is also illustrated in Figure 18. The rapid precession of the molecular symmetry axis about $\vec{J}$ is not affected appreciably by the Stark field. The average value of the molecular dipole moment along $\vec{J}$ couples to the strong external field and causes $\vec{J}$ to precess about the Z-axis at a rapid rate. The nuclear quadrupole moment couples to the average molecular field along the Z-axis causing $\vec{I}$ to precess slowly. The molecular state is satisfactorily specified by the quantum numbers J, K, I, M_J, and M_I. The quantum number M_F can be used, but it is related to M_J and M_I by $M_F = M_J + M_I$. The rotational line is split into Stark levels according to the values of M_J, and the quadrupole coupling gives a hyperfine splitting of each Stark level according to the value of M_I. The hyperfine splitting is small compared to the separation between Stark levels.

In the intermediate field case, the Stark energies and hyperfine energies are comparable in size. In this case, F, M_J, and M_I are not good quantum numbers, and a satisfactory vector diagram for the intermediate case cannot be drawn. Determination of the energy levels is generally rather complex because it involves the diagonalization of the perturbing Hamiltonian $H_Q + H_S$, where H_Q is the quadrupole coupling Hamiltonian and H_S is the Stark effect Hamiltonian.

Chlorotrifluoromethane, $CClF_3$, has the trade name "Freon-13." The sample used in this experiment was obtained from the Matheson Company, and it is reported to have a purity of 99.0 per cent.

The electric dipole moment of $C^{12}Cl^{35}F_3$ was evaluated by Beeson (8) by measuring and analyzing the Stark effect for the $J = 2 \rightarrow 3$ transition. The dipole moment obtained was not considered to be very accurate because of the difficulty of resolving the Stark components. It was decided to revaluate the dipole moment by measuring and analyzing the Stark effect for the $J = 1 \rightarrow 2$ transition since the Stark spectrum is considerably less complex for this transition. Best results were obtained with the Stark cell at dry ice temperature and with a gas pressure of about 0.07 mm of mercury.

In order to determine the energy levels in the presence of the Stark field, it was necessary to determine the eigenvalues of the Hamiltonian matrix, $H_0 + H_Q + H_S$, where H_0 is the unperturbed rotational Hamiltonian and H_Q and H_S are the quadrupole and Stark Hamiltonians, respectively. The matrix elements can be computed from either of two sets of wave functions: (a) the weak field wave functions characterized by J, K, I, F, and M_F or (b) the strong field wave functions characterized by J, K,

I, M_J, and M_I. It appears most convenient to select the latter since expressions for calculating the matrix elements of both H_Q and H_S, for the strong field wave functions, exist in the literature.

Since J, K, and I are good quantum numbers in both the weak and strong field cases, it may be surmised that they are good in the intermediate field case. Thus, the Hamiltonian will be diagonal in J, K, and I; and, for particular values of J, K, and I, the secular equation is

$$\left| < JKIM_JM_I | H_Q + H_S | JKIM_J'M_I' > - W\delta_{M_JM_J'}\delta_{M_IM_I'} \right| = 0 \quad . \tag{40}$$

It may also be surmised that $M_F = M_J + M_I$ is a good quantum number; thus, the Hamiltonian will also be diagonal in M_F. In other words, the Hamiltonian matrix consists of submatrix blocks, dependent on M_F, along the diagonal as illustrated in Figures 19 and 20.

The matrix of the Stark Hamiltonian is diagonal in M_J and M_I; the elements are (36)

$$< JKIM_JM_I | H_S | JKIM_JM_I > = \mu E \frac{KM_J}{J(J+1)} \quad . \tag{41}$$

The matrix elements of the quadrupole Hamiltonian (35) are*

$$< JKIM_JM_I | H_Q | JKIM_J'M_I' >$$

$$= \frac{eqQ}{2I(2I-1)(2J-1)(2J+3)} \left[\frac{3K^2}{J(J+1)} - 1 \right] < M_JM_I | F | M_J'M_I' > \quad , \tag{42}$$

---

* The factor (2J+3) should be included in Equation 2 of Reference 35.

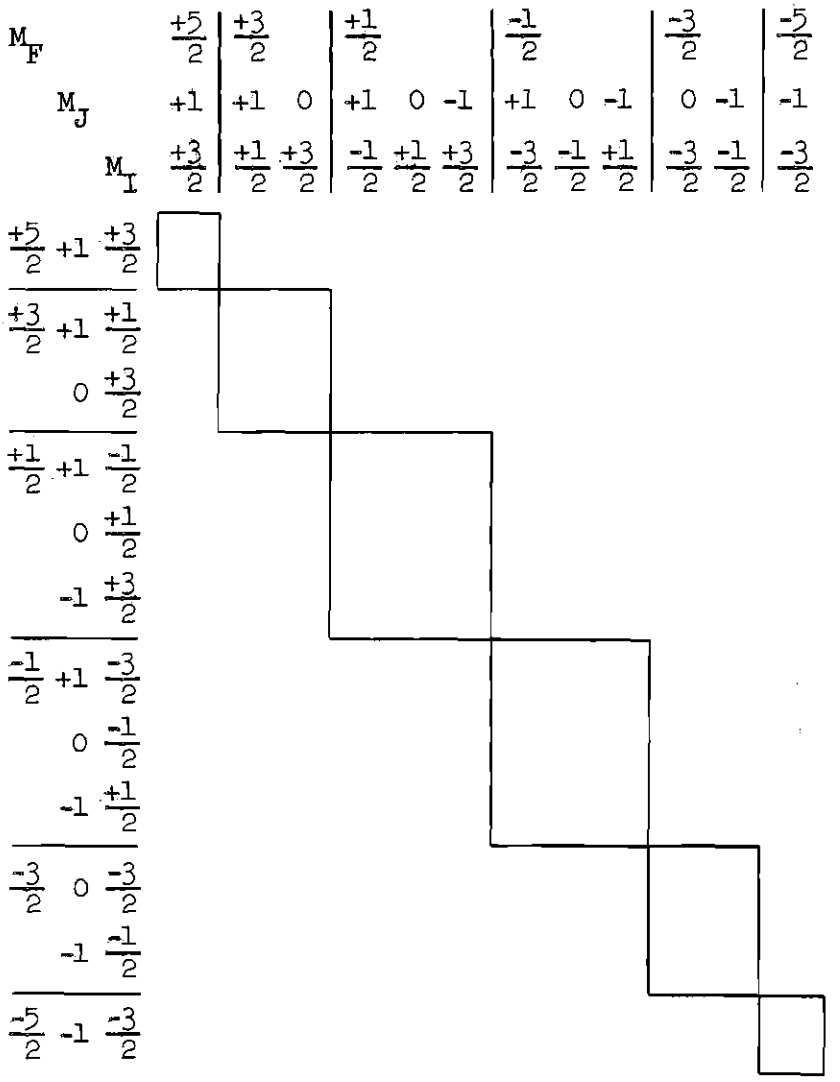

Figure 19. Graphical Illustration of the Hamiltonian Matrix for J = 1, K = 1, and I = 3/2. Non-zero terms appear only in the blocks along the diagonal.

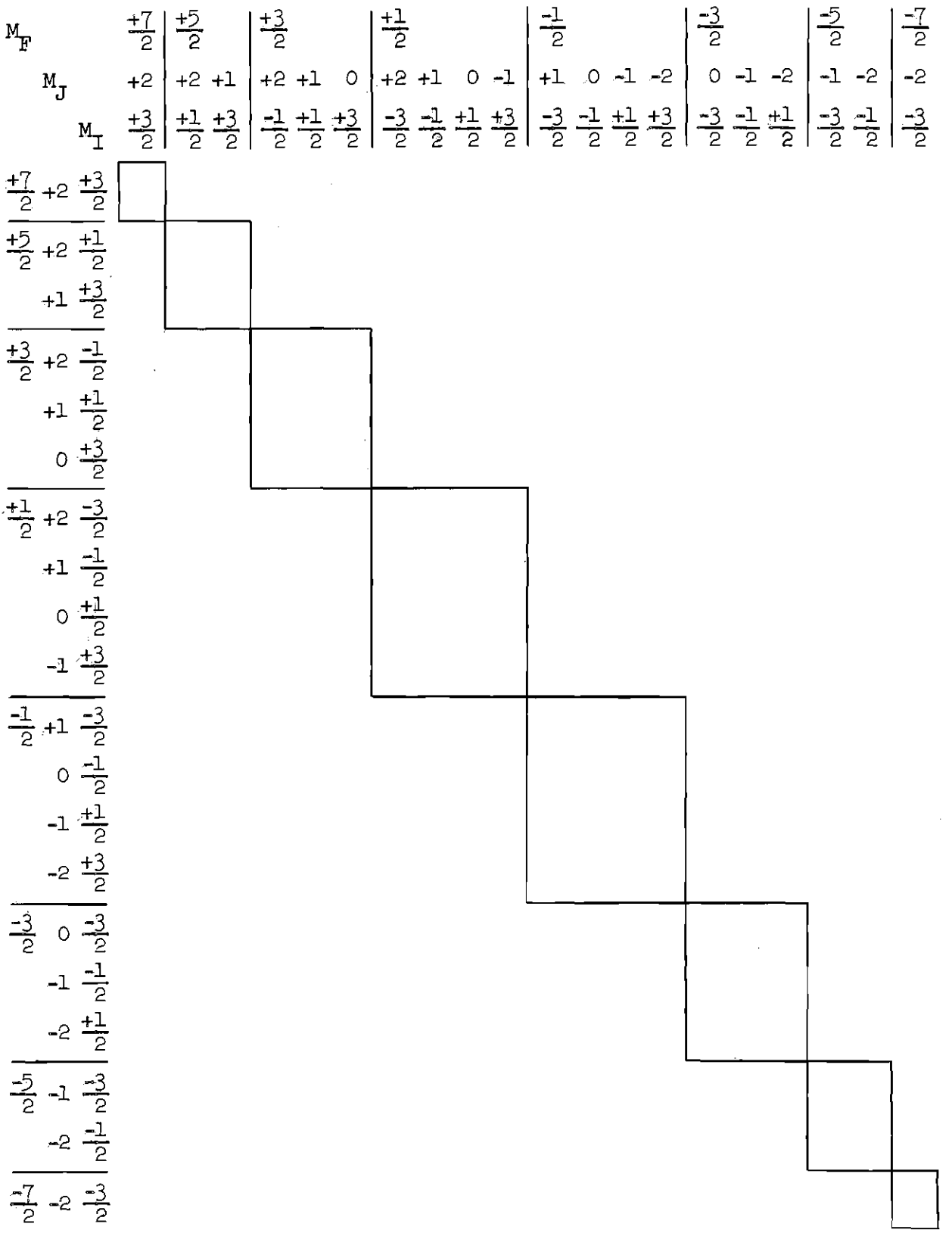

Figure 20. Graphical Illustration of the Hamiltonian Matrix for J = 2, K = 1, and I = 3/2. Non-zero terms appear only in the blocks along the diagonal.

where

$$F = 3(\vec{I} \cdot \vec{J})^2 + \frac{3}{2}(\vec{I} \cdot \vec{J}) - I(I+1)J(J+1) \quad . \tag{43}$$

The operator F has the following nonzero matrix elements (37):

$$< M_J M_I | F | M_J M_I > = \frac{1}{2}\left[3M_I^2 - I(I+1)\right]\left[3M_J^2 - J(J+1)\right] \quad , \tag{44}$$

$$< M_J M_I | F | M_J \mp 1, M_I \pm 1 > = \frac{3}{4}(2M_J \mp 1)(2M_I \pm 1) \tag{45}$$

$$\left[(J \pm M_J)(J \mp M_J + 1)(I \mp M_I)(I \pm M_I + 1)\right]^{1/2} \quad ,$$

and

$$< M_J M_I | F | M_J \mp 2, M_I \pm 2 > = \frac{3}{4}\left[(J \pm M_J)(J \pm M_J - 1)(J \mp M_J + 1)(J \mp M_J + 2)\right. \tag{46}$$

$$\left.(I \mp M_I)(I \mp M_I - 1)(I \pm M_I + 1)(I \pm M_I + 2)\right]^{1/2} \quad .$$

The Hamiltonian matrices for the two cases--(1) J = 1, K = 1, I = 3/2 and (2) J = 2, K = 1, I = 3/2--are illustrated in Figures 19 and 20. The quadrupole coupling constant, eqQ, was assigned the value -77.98 mc, as previously measured by this author, and the molecular electric dipole moment, μ, was assigned the value 0.50 debye* as reported by Beeson (8). The Hamiltonian matrix was calculated for each case at several values of Stark field intensity. The energy eigenvalues were obtained with the aid of an electronic digital computer and the results

---

* 1 debye = 10^{-18} esu cm.

are illustrated in Figures 21 and 22. The electric field intensity in the Stark cell is related to the cell voltage by assuming an electrode spacing of 0.466 cm, as calibrated by measurement of the Stark effect of the OCS molecule.

It appears that the molecule behaves according to the strong field case for field intensities greater than about 400 volts/centimeter; the Stark levels are split according to the values of M_J, and the hyperfine structure is split according to the values of M_I. Recordings of the $J = 1 \rightarrow 2$ transition at various voltages above 400 volts/centimeter indicated a widely separated pair of Stark lines symmetrically located on each side of the group of rotational lines (see Figure 23) as might be expected. Assuming the strong field selection rules for absorption,

$$\begin{aligned} \Delta J &= +1 \\ \Delta K &= 0 \\ \Delta M_J &= 0 \\ \Delta M_I &= 0 \ , \end{aligned} \tag{47}$$

it was found that each Stark line was composed of a group of four unresolved hyperfine lines, and the separation between the groups was a unique function of the electric field intensity.

The evaluation of the molecular dipole moment proceeded then as follows: (a) Stark energy levels versus electric field intensity were calculated, using intermediate field theory (7), for several assumed values of molecular dipole moment in the neighborhood of 0.500 debye. (b) Using the strong field selection rules, a family of curves, one for each assumed value of dipole moment, was constructed illustrating the

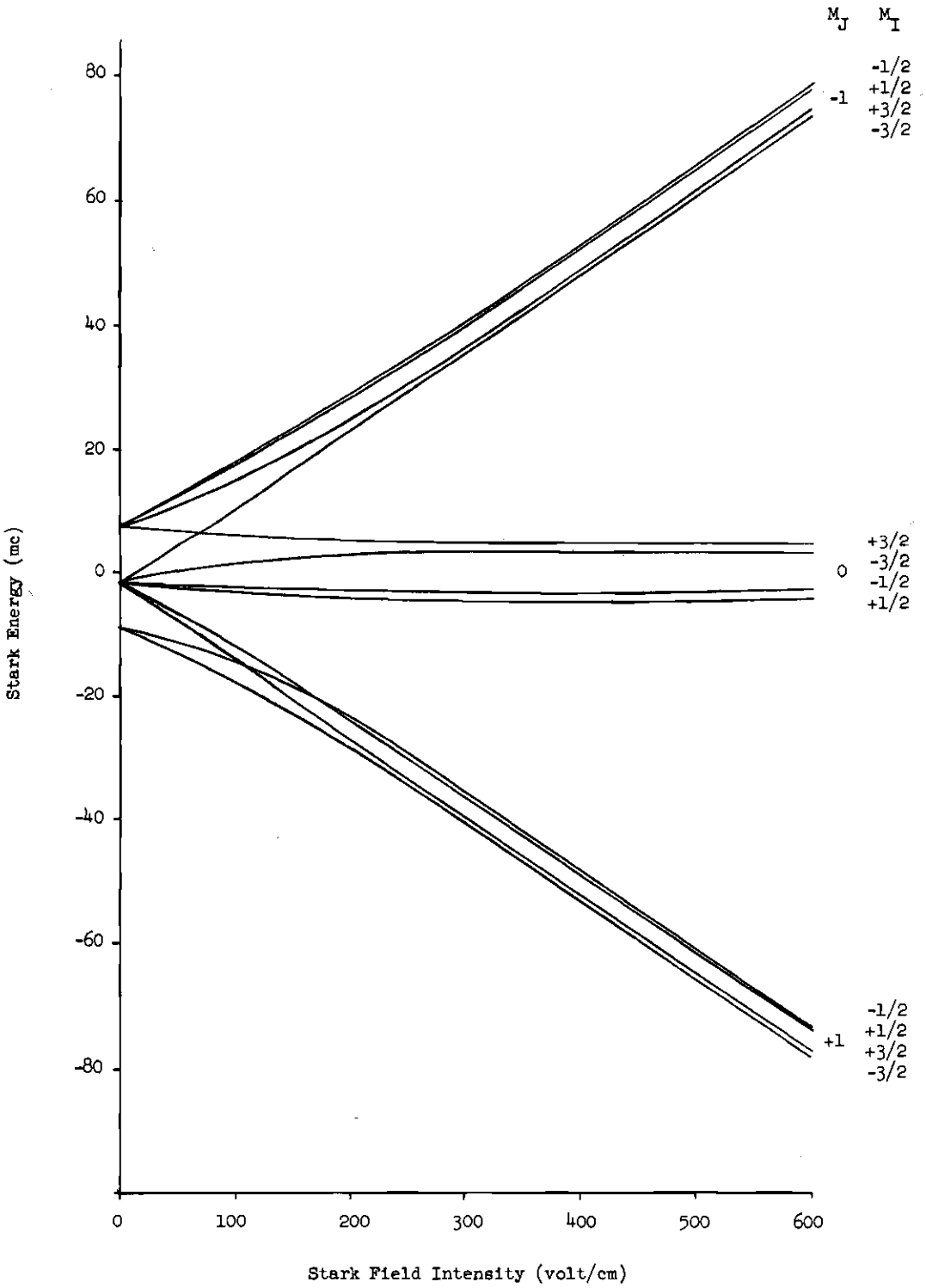

Figure 21. Stark Energy Versus Field Intensity for $C^{12}Cl^{35}F_3$ With J = 1 and K = 1.

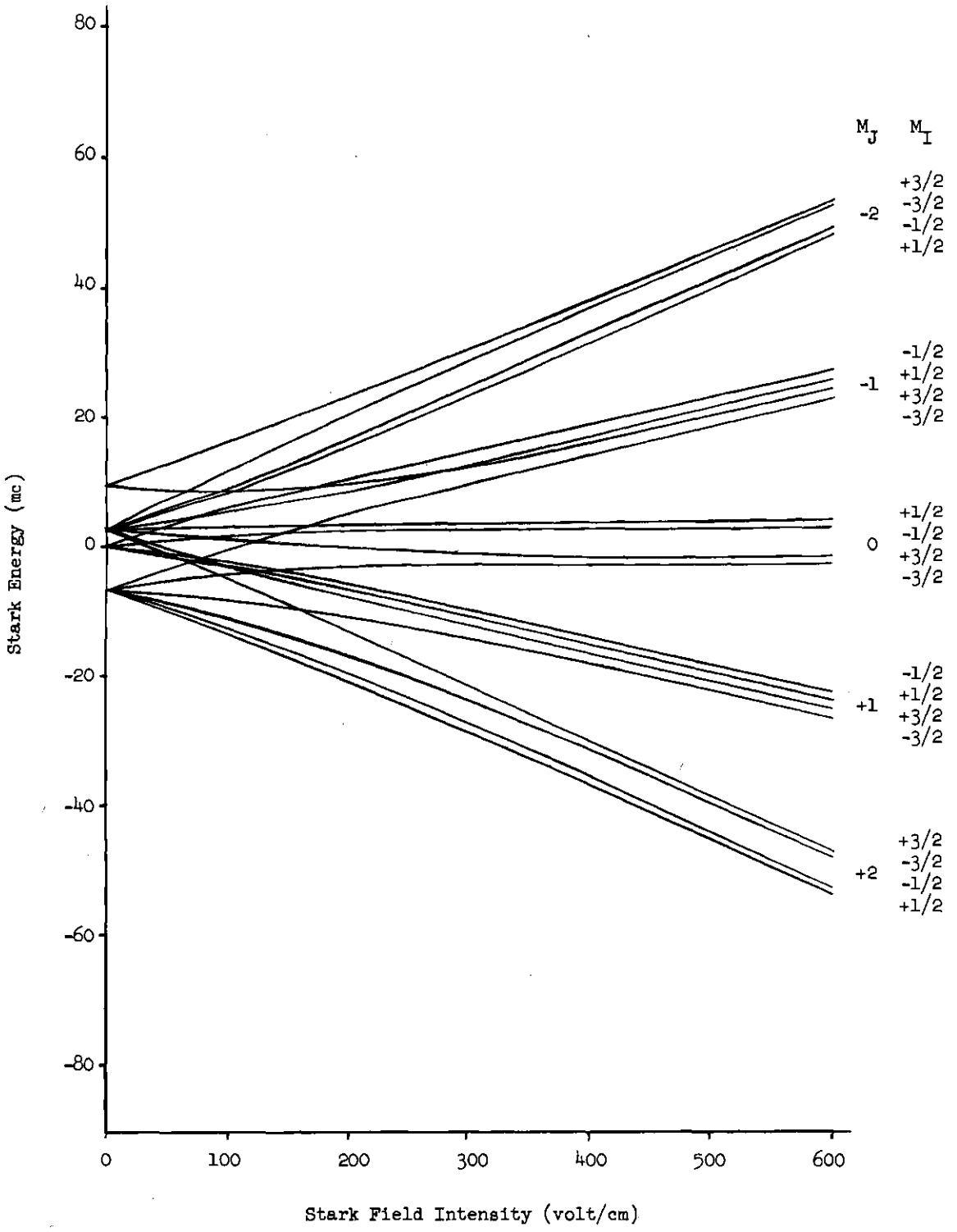

Figure 22. Stark Energy Versus Field Intensity for $C^{12}Cl^{35}F_3$ With J = 2 and K = 1.

Figure 23. Recording of the J = 1→2 Transition of $C^{12}Cl^{35}F_3$ Illustrating Stark Line Separation.

theoretical frequency separation versus field intensity for the pair of Stark lines. Each Stark line was assumed to be the average of its four unresolved hyperfine components. (c) The frequency of each of the pair of Stark lines was accurately measured at two values of electric field intensity: 657 and 1100 volts/centimeter. From these measurements, the frequency separation was found for both values of field intensity. (d) With a large scale graph of the family of curves from Step b and the two experimental points from Step c, the molecular electric dipole moment for $C^{12}Cl^{35}F_3$ was assigned the value

$$\mu = 0.50 \pm 0.01 \text{ debye.} \tag{48}$$

Most of the estimated error in this result is attributed to an uncertainty of the electrode spacing in the Stark cell. A graph of the theoretical Stark line separation versus electric field intensity for the above value of μ, along with the two experimental points, is shown in Figure 24.

The evaluation of μ was essentially independent of the assumed value of eqQ since the quadrupole coupling produced only a small perturbation on the Stark splitting and the individual hyperfine lines were not resolved. By using the measured separation between the pair of Stark lines, the evaluation of μ was made independent of the rotational constant B and effects such as molecular polarization and second-order Stark energies which tend to shift both lines equally in the same direction.

It was desirable, however, to compare the individual measured Stark line frequencies with the theoretical frequencies; the comparison is illustrated in Table 6. The second-order Stark energy (38) was calculated from the equation,

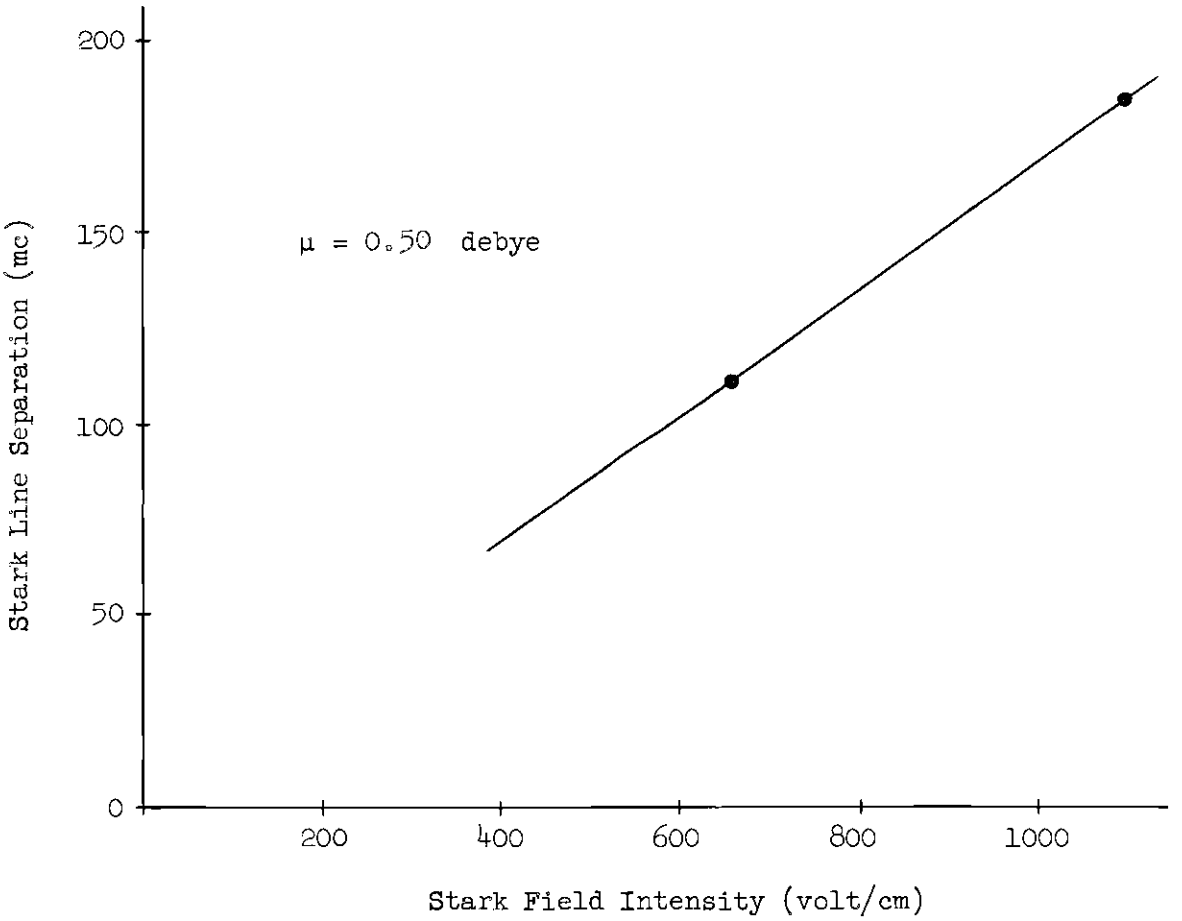

Figure 24. Stark Line Separation Versus Field Intensity for the $J_{3} \equiv 1 \rightarrow 2$, K = 1 Transition of $C^{12}Cl^{35}F_3$.

Table 6. Stark Line Frequencies for $C^{12}Cl^{35}F_3$.[a]

Stark Field Intensity (volt/cm)	M_J	M_I	1st Order Stark Displacement	Average 1st Order Stark Displacement	2nd Order Stark Displacement	Theoretical Stark Line Frequency	Measured Stark Line Frequency
657	+1	+3/2	+56.34				
		+1/2	+54.54				
		-1/2	+55.14				
		-3/2	+55.57	+55.40	+0.33	13,398.1	13,398.2
657	-1	+3/2	-54.37				
		+1/2	-56.20				
		-1/2	-55.71				
		-3/2	-55.30	-55.40	+0.33	13,287.3	13,287.4
1100	+1	+3/2	+93.24				
		+1/2	+91.70				
		-1/2	+92.06				
		-3/2	+92.76	+92.44	+0.94	13,435.7	13,436.1
1100	-1	+3/2	-91.61				
		+1/2	-93.15				
		-1/2	-92.84				
		-3/2	-92.15	-92.44	+0.94	13,250.9	13,251.0

[a] The transitions are $J = 1 \rightarrow 2$, $K = 1$, $I = 3/2$, $\Delta M_J = 0$, $\Delta M_I = 0$; the electric dipole moment is 0.50 debye; the rotational energy is $2B(J+1) = 13,342.40$ mc. Frequencies are given in megacycles.

$$\Delta W_2 = \frac{\mu^2 E^2}{2Bh} \left\{ \frac{(J^2-K^2)(J^2-M_J^2)}{J^3(2J-1)(2J+1)} - \frac{\left[(J+1)^2-K^2\right]\left[(J+1)^2-M_J^2\right]}{(J+1)^3(2J+1)(2J+3)} \right\} . \qquad (49)$$

Polarization of the molecule and higher-order Stark effects were neglected. Comparison of the measured and theoretical frequencies is considered to be quite good since the Stark lines were on the order of three megacycles wide.

CHAPTER VI

CONCLUSIONS AND RECOMMENDATIONS

This investigation of distortion constants was prompted by the recent work (3, 4) on CCl_3F and $CHCl_3$. The results for these molecules were unusual in three respects: (a) the measured values for the rotational distortion constants D_{JJ} and D_{JK} do not agree with the theoretical values calculated from the molecular structure and force constants; (b) the value of D_{JJ} is negative and is a function of J; and (c) the quadrupole coupling constant, assuming extranuclear charge symmetry about the C-Cl bond, is large compared to values observed in other molecules. These two molecules are the only known symmetric tops, having three identical nuclei with quadrupole moments, for which the hyperfine spectra have been analyzed and reported. The centers of mass for these molecules are inside the YZ_3 tetrahedron; whereas the centers of mass for previously reported XYZ_3 molecules, other than CHF_3, are outside the YZ_3 tetrahedron.

The unusual behavior of the distortion constants is particularly disturbing since it is a violation of existing distortion theory, as expressed in Equation 27. For this reason, detailed calculations of distortion constants were made for three other symmetric tops: (a) CH_3Cl, a typical methyl halide; (b) $CClF_3$, a molecule with bonding similar to that of CCl_3F; and (c) CHF_3, a molecule with its center of mass well within the YZ_3 tetrahedron.

The hyperfine absorption spectrum of CH_3Cl has previously been analyzed and reported (16). The resolved hyperfine lines for the $J = 3 \rightarrow 4$

and J = 5→6 transitions were used to calculate distortion constants for all possible combinations of the hypothetical unsplit lines. The molecule was found to obey Equation 27 with no apparent inconsistencies.

The hyperfine absorption spectrum of $CClF_3$ has been reported (17) for the J = 2→3 and J = 3→4 transitions. The hyperfine lines of the J = 1→2 and J = 4→5 transitions were measured in the present work, and all possible combinations of the hypothetical unsplit lines were used to calculate distortion constants. Several inconsistencies were observed for calculations involving the J = 2→3 transition. The J = 2→3 and J = 3→4 transitions were remeasured and compared with the reported values. Good agreement was found for the 3→4 transition; however, slight differences were found for the 2→3 transitions. Using data from the present work, the molecule was found to obey Equation 27 with no apparent inconsistencies. For this reason, the J = 2→3 data reported by Coles and Hughes (17) is believed to be slightly in error. A detailed calculation of distortion constants, for all possible combinations of unsplit lines, appears to be a good method for finding inconsistencies in experimental data.

Based on data from the present investigation for the J = 1→2 through J = 4→5 transitions, the following constants were calculated for $CClF_3$:

$$B = 3335.596 \text{ mc}$$

$$eqQ = - 77.98 \text{ mc}$$

$$D_{JJ} = + 0.59 \text{ kc}$$

$$D_{JK} = + 2.06 \text{ kc} \quad .$$

The absorption spectrum of CHF_3 has previously been analyzed and reported (15). In order to extend the investigation lower in J-values,

the J = 0→1 transition was measured in the present work. Data from the J = 0→1, 3→4, 6→7, and 8→9 transitions were used to calculate distortion constants for all possible combinations of absorption lines. The molecule was found to obey Equation 27 with no apparent inconsistencies.

The theoretical rotational distortion constants for nine symmetric-top molecules were calculated using the molecular structures and the molecular force constants; the former are calculated from microwave spectra and the latter are calculated from Raman and infrared spectra. A comparison of the theoretical and observed distortion constants provides an interesting link between spectra in the microwave and infrared regions. Agreement between the calculated and the observed constants was fair for all molecules considered except $CHCl_3$ and CCl_3F.

From a Taylor's expansion of the energy, expressed as a function of J and K, it is clear that all molecules should have constant distortion coefficients, particularly if additional terms are included as in Equation 28. An attempt was made to fit the reported CCl_3F data using distortion constants through second order; however, the data were found to be inconsistent.

All molecules considered in this investigation, except $CHCl_3$ and CCl_3F, obey existing distortion theory and show fair agreement with infrared data. The two exceptional molecules, $CHCl_3$ and CCl_3F, should be studied further; and, in particular, the theory of quadrupole interaction involving three identical nuclei with spin 3/2 should be re-examined.

The dipole moment of $C^{12}Cl^{35}F_3$ was evaluated by measuring and analyzing the Stark effect for the J = 1→2 transition; the result was

$$\mu = 0.50 \pm 0.01 \text{ debye.}$$

By measuring the separation between the pair of strong Stark lines at various electric field intensities, the results were made independent of the quadrupole coupling constant, second-order Stark effects, and molecular polarization. Most of the estimated error in the evaluation of the dipole moment is the result of an uncertainty of the electrode spacing in the Stark cell. A more accurate calibration of the electrode spacing would enable a more significant evaluation of the dipole moment.

In the present work, an electronic digital computer was utilized to calculate the theoretical distortion constants and to diagonalize matrices in the study of the Stark effect in $CClF_3$. Many of the standard calculations in microwave spectroscopy, although simple in principle, are laborious to carry out. It is felt that several of these calculations can be handled conveniently with electronic computer routines. For example, the theoretical absorption frequencies for symmetric-top molecules can be calculated from the constants B, eqQ, D_{JJ}, and D_{JK} or the constants can be evaluated from the measured absorption frequencies. Utilizing computer routines can free the experimenter from many of the time-consuming calculations.

APPENDIX A

DISTORTION COEFFICIENTS

Centrifugal stretching of symmetric tops is somewhat complicated because it involves both angular momentum quantum numbers J and K. The problem can be handled quite simply, however, if the following three assumptions are made.

(1) Assume that each energy level (neglecting quadrupole interactions) for a nonrigid rotor is determined by the quantum numbers J and K. The total energy is the sum of the kinetic energy of rotation of the distorted molecule and the potential energy stored in the stretched bonds; however, each of these are functions of J and K. Hence, the total energy for each level is determined by J and K.

(2) Assume that the amount of centrifugal distortion of the molecule does not depend on the sign of the angular rotation (e.g., whether it is clockwise or counterclockwise). Then, the energy levels must be functions of only even powers of the momentum, such as the square of the total angular momentum $J(J+1)\hbar^2$ or the square of the component of momentum along the symmetry axis $K^2\hbar^2$.

(3) Assume that the total energy function $W'\left[J(J+1),K^2\right]$, where $W' = W/h$ is the energy expressed in units of frequency, is analytic at the origin ($J = 0$ and $K = 0$) and that quantum mechanics specifies the allowed values of J and K.

In order to simplify the notation, make the following associations:

$$x \rightarrow J(J+1) \tag{50}$$

$$y \rightarrow K^2 \quad .$$

Then, use Taylor's theorem to make an expansion about the origin (i.e., $J = 0$, $K = 0$). The result is

$$W'(x,y) = W'_o + W'_x x + W'_y y \tag{51}$$

$$+ \frac{1}{2} W'_{xx} x^2 + W'_{xy} xy + \frac{1}{2} W'_{yy} y^2$$

$$+ \frac{1}{6} W'_{xxx} x^3 + \frac{1}{2} W'_{xxy} x^2 y + \frac{1}{2} W'_{xyy} xy^2 + \frac{1}{6} W'_{yyy} y^3 + \cdots \quad ,$$

where, for example, $W'_x = (\partial W'/\partial x)$ evaluated at $x = 0$ and $y = 0$.

The constant term W'_o may arbitrarily be set equal to zero. Identify the various derivatives in the following manner:

$$W'_x \rightarrow B$$

$$W'_y \rightarrow A - B$$

$$W'_{xx} \rightarrow -2D_{JJ}$$

$$W'_{xy} \rightarrow -D_{JK}$$

$$W'_{yy} \rightarrow -2D_{KK}$$

$$W'_{xxx} \rightarrow -6D_{JJJ}$$

$$W'_{xxy} \rightarrow -2D_{JJK}$$

$$W'_{xyy} \rightarrow -2D_{JKK}$$

$$W'_{yyy} \rightarrow -6D_{KKK}, \text{ etc.}$$

Then, the energy of the level, specified by the quantum numbers J and K, can be expressed as

$$W' = \frac{W}{h} = J(J+1)B + K^2(A-B) \qquad (52)$$
$$- J^2(J+1)^2D_{JJ} - J(J+1)K^2D_{JK} - K^4D_{KK}$$
$$- J^3(J+1)^3D_{JJJ} - J^2(J+1)^2K^2D_{JJK} - J(J+1)K^4D_{JKK}$$
$$- K^6D_{KKK} + \ldots \ .$$

In the expansion of the energy function W', A and B are first-order coefficients; D_{JJ}, D_{JK}, and D_{KK} are second-order coefficients; D_{JJJ}, D_{JJK}, D_{JKK}, and D_{KKK} are third-order coefficients; etc. In the field of microwave spectroscopy, A and B are defined as rotational constants; D_{JJ}, D_{JK}, and D_{KK} are defined as distortion constants; and other D's are referred to as higher-order distortion constants. In order to be more specific when referencing distortion constants, the following definitions have been used here: A and B are rotational constants; D_{JJ}, D_{JK}, and D_{KK} are first-order distortion constants; D_{JJJ}, D_{JJK}, D_{JKK}, and D_{KKK} are second-order distortion constants; etc. Defining the order of the distortion constants in this manner seems to be the most satisfactory method, even though the order of the distortion constant does not correspond to the order of the coefficient in the expansion, Equation 52.

The energy of the level specified by J+1 and K can be expressed in a manner similar to Equation 52. Then, the frequency for the transition $J \rightarrow J+1$ and $\Delta K = 0$ can be expressed as

$$\nu = 2(J+1)B - 4(J+1)^3D_{JJ} - 2(J+1)K^2D_{JK} \qquad (53)$$
$$- 2(J+1)^3(3J^2+6J+4)D_{JJJ} - 4(J+1)^3K^2D_{JJK} - 2(J+1)K^4D_{JKK} + \ldots \ ,$$

which is identical to that given by Costain (39). It is often more

convenient to divide both sides by 2(J+1) which yields

$$\frac{\nu}{2(J+1)} = B - 2(J+1)^2 D_{JJ} - K^2 D_{JK} \qquad (54)$$
$$- (J+1)^2(3J^2+6J+4)D_{JJJ} - 2(J+1)^2K^2D_{JJK} - K^4D_{JKK} + \ldots \quad .$$

It should be noted that B and the D's are constants by definition. If the basic assumptions are valid, any spectrum (neglecting quadrupole interactions) can be represented by Equation 54 if enough terms are included; usually the first three terms are sufficient.

APPENDIX B

BOND ANGLES IN XYZ_3 MOLECULES

Consider an XYZ_3 molecule as illustrated in Figure 25. Using elementary trigonometric formulae for triangles, the following are obtained:

$$\cos \alpha = \frac{2d^2 - 3a^2}{2d^2} \tag{55}$$

$$\cos \beta = \frac{-b}{d} \tag{56}$$

$$\cos \gamma = \frac{b}{d} \quad . \tag{57}$$

Since $a^2 = d^2 - b^2$,

$$\cos \alpha = \frac{3b^2 - d^2}{2d^2} \quad . \tag{58}$$

From Equations 57 and 58, the angles α and γ are related as follows:

$$\cos \alpha = \frac{3 \cos^2 \gamma - 1}{2} \tag{59}$$

$$\cos \gamma = \sqrt{\frac{2 \cos \alpha + 1}{3}} \tag{60}$$

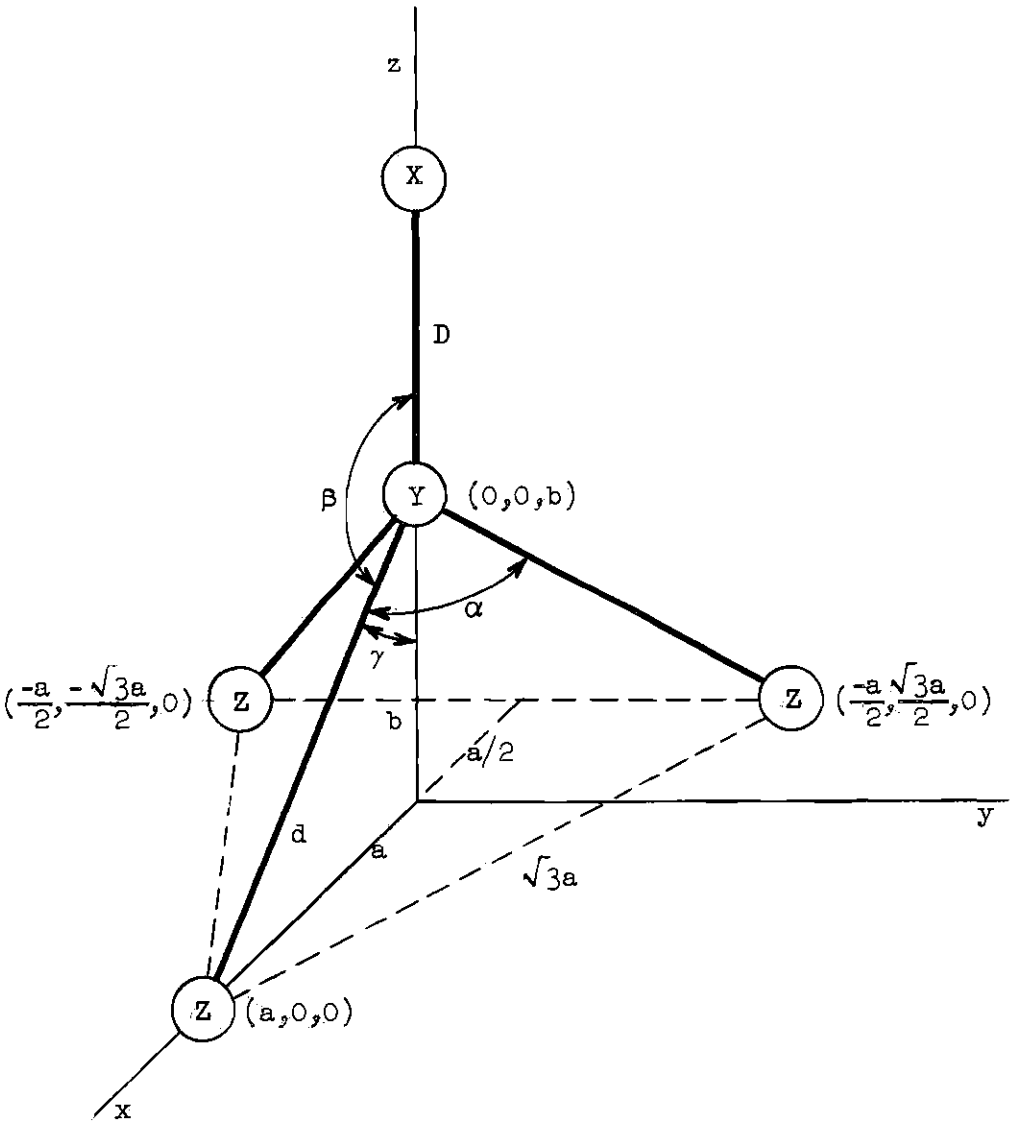

Figure 25. Bond Angles in an XYZ_3 Molecule.

APPENDIX C

MOMENTS OF INERTIA IN XYZ_3 MOLECULES

Consider an XYZ_3 molecule with fixed bond lengths and a configuration as illustrated in Figure 26. The moments of inertia can be expressed as a function of the angle γ.

The location of the center of mass is

$$\ell = \frac{3m_Z b - m_X D}{M} \quad , \tag{61}$$

where $M = m_X + m_Y + 3m_Z$. The moment of inertia about the y-axis is

$$I_{yy} = m_X(D+\ell)^2 + m_Y\ell^2 + 3m_Z(b-\ell)^2 + \frac{3}{2} m_Z a^2 \quad . \tag{62}$$

From Equations 61 and 62 and the relations $a = d \sin\gamma$ and $b = d \cos\gamma$, I_{yy} can be expressed as a function of γ; the result is

$$I_{yy} = \left(m_X D^2 + \frac{3}{2} m_Z d^2 - \frac{m_X^2 D^2}{M}\right) + \left(\frac{6m_Z m_X dD}{M}\right) \cos\gamma \tag{63}$$

$$+ \left(\frac{3}{2} m_Z d^2 - \frac{9m_Z^2 d^2}{M}\right) \cos^2\gamma \quad .$$

The moment of inertia about the z-axis is

$$I_{zz} = 3m_Z a^2 \tag{64}$$

or

$$I_{zz} = 3m_Z d^2 \sin^2\gamma \quad . \tag{65}$$

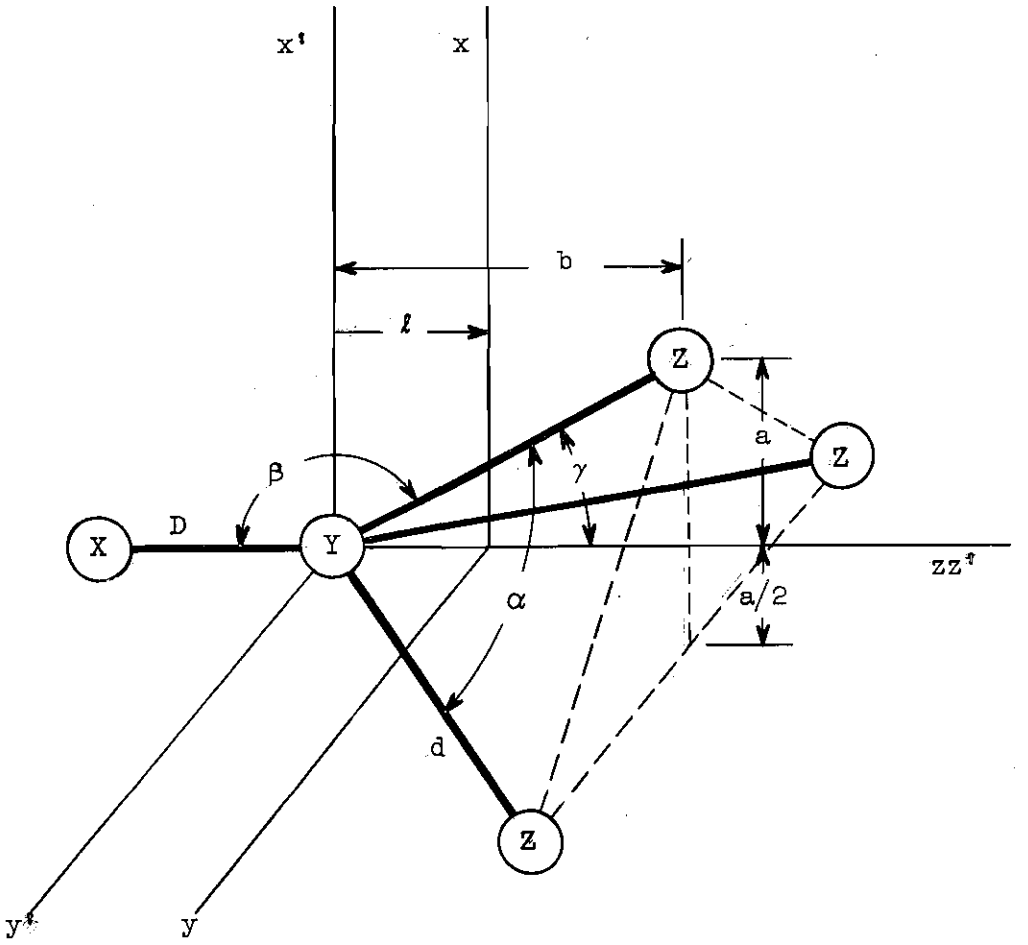

Figure 26. Structural Parameters of an XYZ_3 Molecule.

The derivatives of the moments of inertia with respect to γ are

$$\frac{dI_{yy}}{d\gamma} = 6m_Z d\left(\ell - \frac{b}{2}\right) \sin \gamma \qquad (66)$$

and

$$\frac{dI_{zz}}{d\gamma} = 6m_Z d^2 \sin \gamma \cos \gamma \quad . \qquad (67)$$

From Equation 67, it is seen that I_{zz} increases with γ as expected. From Equation 66, however, it is seen that I_{yy} increases with γ if ℓ is greater than b/2; but it decreases with an increase of γ if ℓ is less than b/2. Centrifugal forces due to rotation about any given axis will always tend to increase the moment of inertia about that axis. Therefore, rotation about an axis perpendicular to the molecular symmetry axis will tend to increase the angle γ if the center of mass is in the lower half ($\ell > b/2$) of the YZ_3 tetrahedron, and it will tend to decrease the angle γ if the center of mass is above the mid-point ($\ell < b/2$) of the YZ_3 tetrahedron.

APPENDIX D

HYBRIDIZATION WITH QUADRICOVALENT ATOMS

Stable bonds are formed only with the use of stable atomic orbitals--the 1s orbital for hydrogen, the 2s and 2p orbitals for the first-row atoms, and so on. The various stable orbitals of an atom which can be used for bond formation do not differ much in their radial dependence; however, they may show a great difference in their angular distribution. For tetrahedral bond orbitals, the angular parts of the wave functions are

$$\begin{aligned} s &= 1 \\ p_x &= 3 \sin\theta \cos\phi \\ p_y &= 3 \sin\theta \sin\phi \\ p_z &= 3 \cos\theta \quad , \end{aligned} \tag{68}$$

where θ and ϕ are the angles in spherical polar angles. These functions are normalized to 4π: the integral of the square of the function taken over the surface of the unit sphere has the value 4π.

Treating the electronic wave functions as vectors, the hybrid bond functions can be written as

$$\begin{aligned} \phi_1 &= d_1 s + cp_z \\ \phi_2 &= d_2 s + ap_x - bp_z \\ \phi_3 &= d_2 s - \frac{a}{2} p_x + \frac{\sqrt{3}}{2} ap_y - bp_z \\ \phi_4 &= d_2 s - \frac{a}{2} p_x - \frac{\sqrt{3}}{2} ap_y - bp_z \quad , \end{aligned} \tag{69}$$

where a, b, c, d_1, and d_2 are arbitrary constants. Requiring the wave functions to be orthonormal and evaluating the coefficients results in

$$\phi_1 = \frac{\sqrt{2}}{\tan \gamma} s + \sqrt{1 - \frac{2}{\tan^2 \gamma}}\, p_z \qquad (70)$$

$$\phi_2 = \sqrt{\frac{1}{3} - \frac{2}{3 \tan^2 \gamma}}\, s + \sqrt{\frac{2}{3}}\, p_x - \frac{\sqrt{2/3}}{\tan \gamma}\, p_z$$

$$\phi_3 = \sqrt{\frac{1}{3} - \frac{2}{3 \tan^2 \gamma}}\, s - \frac{1}{2}\sqrt{\frac{2}{3}}\, p_x + \frac{\sqrt{2}}{2}\, p_y - \frac{\sqrt{2/3}}{\tan \gamma}\, p_z$$

$$\phi_4 = \sqrt{\frac{1}{3} - \frac{2}{3 \tan^2 \gamma}}\, s - \frac{1}{2}\sqrt{\frac{2}{3}}\, p_x - \frac{\sqrt{2}}{2}\, p_y - \frac{\sqrt{2/3}}{\tan \gamma}\, p_z \quad .$$

From Appendix B,

$$\cos \gamma = \frac{1 + 2 \cos \alpha}{3}$$

or

$$\tan^2 \gamma = \frac{2 - 2 \cos \alpha}{1 + 2 \cos \alpha} \quad . \qquad (71)$$

Therefore, the percentage of hybridization in the Y-Z bonds is

$$\frac{1}{3}\left(1 - \frac{1 + 2 \cos \alpha}{1 - \cos \alpha}\right) 100\% \quad , \qquad (72)$$

as illustrated in Figure 27. Hybridization for tetrahedral bond angles is 25 per cent; if the YZ_3 atoms form a planar structure, the hybridization is 33 per cent.

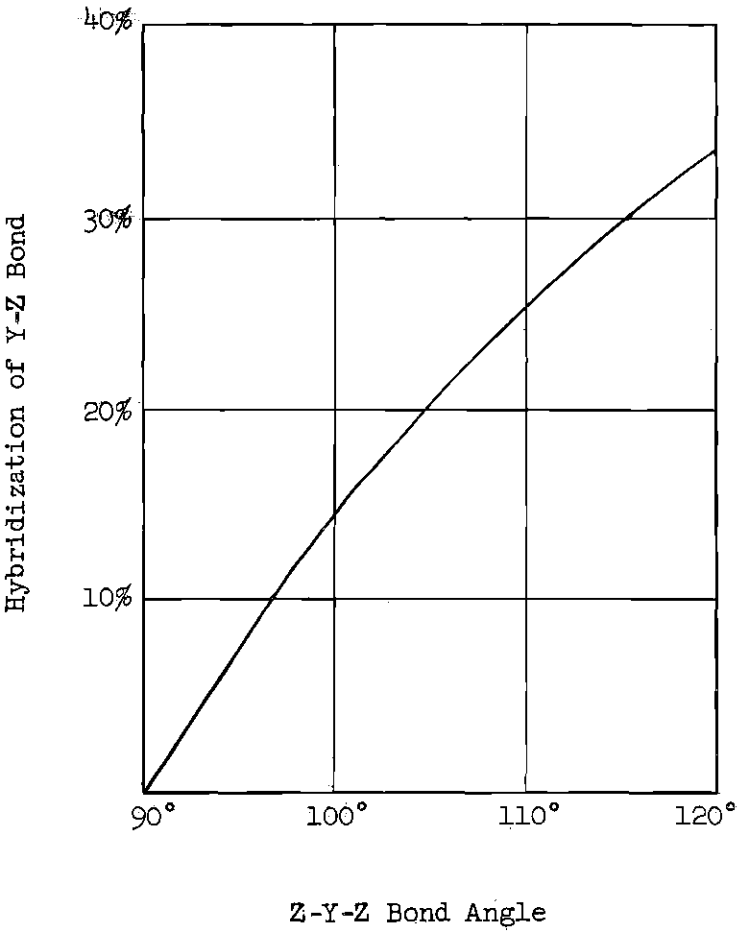

Figure 27. Hybridization in XYZ_3 Molecules

APPENDIX E

TABLES FOR CALCULATION OF ROTATIONAL DISTORTION CONSTANTS

Table 7. The $\left[J^i_{\alpha\beta}\right]_o$ for an Axially Symmetric XYZ_3 Molecule.[a,b]

i	$\left[J^i_{xx}\right]_o$	$\left[J^i_{zz}\right]_o$	$\left[J^i_{xz}\right]_o$
R_1	$2m_1(D+\ell)$	0	0
R_2	$\sqrt{3}m_3\left(d(1+c^2)+2\ell c\right)$	$2\sqrt{3}m_3 ds^2$	0
R_3	$\sqrt{6}m_3 dsk\left(\frac{dc}{2}+\ell\right)$	$-\sqrt{6}m_3 d^2 sck$	0
R_{1a}	$\frac{-\sqrt{6}}{2} m_3 ds^2$	0	$-\sqrt{6}m_3 s(dc+\ell I^x_{yy})$
R_{2a}	0	0	$\frac{\sqrt{6}}{3} m_1 D(D+\ell)2I^x_{yy}$
R_{3a}	$\frac{\sqrt{2}}{2} m_3 d^2 s^2 \Gamma$	0	$-\sqrt{2}m_3 ds\Gamma(dc+\ell)I^x_{yy}$
R_{1b}, R_{2b}, R_{3b}	0	0	0

[a] From References 5 and 6. Some of the symbols have been changed for this presentation.

[b] The symbols are defined as follows: $c = \cos\beta$; $s = \sin\beta$; β = X-Y-Z angle; m_1 = mass of X atom; m_3 = mass of Z atom; D = X-Y bond distance; d = Y-Z bond distance; $\Gamma = \sec\delta$, where δ is the angle between the X-Y bond and the normal to the Z-Y-Z plane; $\delta = \frac{\pi}{2} - \arctan\left(\frac{\sin\beta}{2\cos\beta}\right)$; $\ell = -M^{-1}(m_1 D + 3m_3 d\cos\beta)$; $M = \Sigma_i m_i$; $I^x_{yy} = I_x I^{-1}_{yy}$, where $I_x = \Sigma_i m_i x_i^2$; and $k = -\frac{\cos\alpha/2}{\sqrt{3}\cos\beta}$, where α = Z-Y-Z angle.

Table 8. Force Constant Symbols for XCZ_3 Molecules.[a]

f_x	f_D	C-X stretching
f_z	f_d	C-Z stretching
f_{zz}	f_α	Z-C-Z bending
f_{xz}	f_β	X-C-Z bending
f_x^z	f_{Dd}	C-X, C-Z interaction
f_x^{zz}	$f_{D\alpha}$	C-X, Z-C-Z interaction
f_x^{xz}	$f_{D\beta}$	C-X, X-C-Z interaction
f_z^z	f_{dd}	C-Z interaction between different bonds
f_z^{zz}	$f_{d\alpha}$	C-Z, Z-C-Z interaction with C-Z forming one side of angle
$f_z^{zz'}$, $f_{z'}^{zz}$	$f_{d\alpha}'$	C-Z, Z-C-Z interaction with C-Z different from bonds forming angle
f_z^{xz}	$f_{d\beta}$	C-Z, X-C-Z interaction with C-Z forming one side of angle
$f_z^{xz'}$	$f_{d\beta}'$	C-Z, X-C-Z interaction with C-Z different from bonds forming angle
f_{zz}^{xz}	$f_{\alpha\beta}$	X-C-Z, Z-C-Z interaction with C-Z bond common to both angles
$f_{zz}^{xz'}$	$f_{\alpha\beta}'$	X-C-Z, Z-C-Z interaction with no bond common to both angles
$f_{zz}^{zz'}$	$f_{\alpha\alpha}$	Z-C-Z interaction
$f_{xz}^{xz'}$	$f_{\beta\beta}$	X-C-Z interaction

[a] The xz symbolism is more recent; it was introduced in Reference 40. All force constants in the $Dd\alpha\beta$ symbolism are in units of md/A; to convert numerically to the more modern xz symbolism, bond stretching and bond interactions go directly, multiply bond angle interactions by d, and multiply angle bending and angle interactions by d^2, where d is the equilibrium length of the C-Z bond.

Table 9. The f Matrix.[a]

	Δx	Δz_1	Δz_2	Δz_3	Δxz_1	Δxz_2	Δxz_3	Δzz_{12}	Δzz_{23}	Δzz_{31}
Δx	f_x	f_x^z	f_x^z	f_x^z	f_x^{xz}	f_x^{xz}	f_x^{xz}	f_x^{zz}	f_x^{zz}	f_x^{zz}
Δz_1		f_z	f_z^z	f_z^z	f_z^{xz}	$f_z^{xz'}$	$f_z^{xz'}$	f_z^{zz}	$f_z^{zz'}$	f_z^{zz}
Δz_2			f_z	f_z^z	$f_z^{xz'}$	f_z^{xz}	$f_z^{xz'}$	f_z^{zz}	f_z^{zz}	$f_z^{zz'}$
Δz_3				f_z	$f_z^{xz'}$	$f_z^{xz'}$	f_z^{xz}	$f_z^{zz'}$	f_z^{zz}	f_z^{zz}
Δxz_1					f_{xz}	$f_{xz}^{xz'}$	$f_{xz}^{xz'}$	f_{zz}^{xz}	$f_{zz}^{xz'}$	f_{zz}^{xz}
Δxz_2						f_{xz}	$f_{xz}^{xz'}$	f_{zz}^{xz}	f_{zz}^{xz}	$f_{zz}^{xz'}$
Δxz_3							f_{xz}	$f_{zz}^{xz'}$	f_{zz}^{xz}	f_{zz}^{xz}
Δzz_{12}								f_{zz}	$f_{zz}^{zz'}$	$f_{zz}^{zz'}$
Δzz_{23}									f_{zz}	$f_{zz}^{zz'}$
Δzz_{31}										f_{zz}

[a] The matrix is symmetric.

Table 10. The U and $U^{\dagger}$ Matrices.

$$U_{A1} = \begin{bmatrix} 1 & 0 & 0 & 0 & 0 & 0 & 0 & 0 & 0 & 0 \\ 0 & 1/\sqrt{3} & 1/\sqrt{3} & 1/\sqrt{3} & 0 & 0 & 0 & 0 & 0 & 0 \\ 0 & 0 & 0 & 0 & -1/\sqrt{6} & -1/\sqrt{6} & -1/\sqrt{6} & 1/\sqrt{6} & 1/\sqrt{6} & 1/\sqrt{6} \end{bmatrix}$$

$$U_{E} = \begin{bmatrix} 0 & 0 & 1/\sqrt{2} & -1/\sqrt{2} & 0 & 0 & 0 & 0 & 0 & 0 \\ 0 & 0 & 0 & 0 & 0 & 1/\sqrt{2} & -1/\sqrt{2} & 0 & 0 & 0 \\ 0 & 0 & 0 & 0 & 0 & 0 & 0 & -1/\sqrt{2} & 0 & 1/\sqrt{2} \end{bmatrix}$$

$$U_{A1}^{\dagger} = \begin{bmatrix} 1 & 0 & 0 \\ 0 & 1/\sqrt{3} & 0 \\ 0 & 1/\sqrt{3} & 0 \\ 0 & 1/\sqrt{3} & 0 \\ 0 & 0 & -1/\sqrt{6} \\ 0 & 0 & -1/\sqrt{6} \\ 0 & 0 & -1/\sqrt{6} \\ 0 & 0 & 1/\sqrt{6} \\ 0 & 0 & 1/\sqrt{6} \\ 0 & 0 & 1/\sqrt{6} \end{bmatrix} \qquad U_{E}^{\dagger} = \begin{bmatrix} 0 & 0 & 0 \\ 0 & 0 & 0 \\ 1/\sqrt{2} & 0 & 0 \\ -1/\sqrt{2} & 0 & 0 \\ 0 & 0 & 0 \\ 0 & 1/\sqrt{2} & 0 \\ 0 & -1/\sqrt{2} & 0 \\ 0 & 0 & -1/\sqrt{2} \\ 0 & 0 & 0 \\ 0 & 0 & 1/\sqrt{2} \end{bmatrix}$$

Table 11. The F Matrix.[a]

For type A_1 vibrations:

	R_1	R_2	R_3
R_1	f_x	$\sqrt{3}f_x^z$	$\frac{\sqrt{6}}{2}\left(f_x^{zz} - f_x^{xz}\right)$
R_2		$f_z + 2f_z^z$	$\frac{\sqrt{2}}{2}\left(2f_z^{zz} + f_z^{zz'} - 2f_z^{xz'} - f_z^{xz}\right)$
R_3			$\frac{1}{2}\left(f_{zz} + f_{xz} + 2f_{xz}^{xz'} + 2f_{zz}^{zz'} - 2f_{zz}^{xz'} - 4f_{xz}^{zz}\right)$

For type E vibrations:[b]

	R_{1a}	R_{2a}	R_{3a}
R_{1a}	$f_z - f_z^z$	$f_z^{xz} - f_z^{xz'}$	$f_z^{zz'} - f_z^{zz}$
R_{2a}		$f_{xz} - f_{xz}^{xz'}$	$f_{zz}^{xz'} - f_{zz}^{xz}$
R_{3a}			$f_{zz} - f_{zz}^{zz'}$

[a] Both submatrices are symmetric.

[b] The same submatrix is obtained for R_{1b}, R_{2b}, and R_{3b}.

BIBLIOGRAPHY

1. Z. I. Slawsky and D. M. Dennison, "The Centrifugal Distortion of Axial Molecules," Journal of Chemical Physics 7, 509-521 (1939).

2. C. H. Townes and A. L. Schawlow, Microwave Spectroscopy, McGraw-Hill Book Company, Inc., 1955, p. 79.

3. M. W. Long, Q. Williams, and T. L. Weatherly, "Microwave Spectrum of $CFCl_3$," Journal of Chemical Physics 33, 508-516 (1960).

4. M. W. Long, "Centrifugal Distortion in Symmetric Top Molecules," Journal of Chemical Physics 32, 948 (1960).

5. J. M. Dowling, R. Gold, and A. G. Meister, "Calculation of Rotational Distortion Constants for Some Axially Symmetric ZX_3Y Molecules," Journal of Molecular Spectroscopy 1, 265-269 (1957).

6. J. M. Dowling, R. Gold, and A. G. Meister, "A Note on the Calculation of Rotational Distortion Constants for Axially Symmetric ZX_3Y Molecules," Journal of Molecular Spectroscopy 2, 411-412 (1958).

7. G. Birnbaum, "Nonresonant Absorption of Symmetric Top Molecules," Journal of Chemical Physics 27, 360-368 (1957).

8. E. L. Beeson, The Microwave Spectrum of $CHClF_2$ and the Stark Effect of $CHClF_2$, $CClF_3$ and NOCl, Unpublished Ph.D. Thesis, Georgia Institute of Technology, June 1960, p. 50.

9. R. H. Hughes and E. B. Wilson, "A Microwave Spectrograph," Physical Review 71, 562 (1947).

10. D. M. Dennison, "The Rotation of Molecules," Physical Review 28, 318-333 (1926).

11. F. Reiche and H. Rademacher, "The Quantum Levels of Symmetric Tops According to Schrodinger's Wave Mechanics," Zeitschrift Für Physik 39, 444-446 (1927).

12. R. de L. Kronig and I. I. Rabi, "The Symmetric Top in the Undulatory Mechanics," Physical Review 29, 262-269 (1927).

13. Townes and Schawlow, op. cit., p. 154.

14. Ibid., Appendix I, p. 499.

15. C. A. Burrus and W. Gordy, "Spectra of Some Symmetric-Top Molecules in the One- to Four-Millimeter Wave Region," Journal of Chemical Physics 26, 391-394 (1957).

16. W. J. O. Thomas, J. T. Cox, and W. Gordy, "Millimeter Wave Spectra and Centrifugal Stretching Constants of the Methyl Halides," Journal of Chemical Physics 22, 1718-1722 (1954).

17. D. K. Coles and R. H. Hughes, Molecular Microwave Spectra Tables, Compiled by P. Kisluik and C. H. Townes, National Bureau of Standards Circular 518, 23 June 1952, p. 9.

18. E. B. Wilson and J. B. Howard, "The Vibration-Rotation Energy Levels of Polyatomic Molecules," Journal of Chemical Physics 4, 260-268 (1936).

19. A. G. Meister, F. F. Cleveland, and M. J. Murray, "Interpretation of the Spectra of Polyatomic Molecules by Use of Group Theory," American Journal of Physics 11, 239-247 (1943).

20. J. E. Rosenthal and G. M. Murray, "Group Theory and the Vibrations of Polyatomic Molecules," Reviews of Modern Physics 8, 317-346 (1936).

21. A. G. Meister and F. F. Cleveland, "Application of Group Theory to the Calculation of Vibrational Frequencies of Polyatomic Molecules," American Journal of Physics 14, 13-27 (1946).

22. S. N. Ghosh, R. Trambarulo, and W. Gordy, "Microwave Spectra and Molecular Structures of Fluoroform, Chloroform and Methyl Chloroform," Journal of Chemical Physics 20, 605-607 (1952).

23. S. L. Miller, L. C. Aamodt, G. Dousmanis, and C. H. Townes, "Structure of the Methyl Haldies," Journal of Chemical Physics 20, 1112-1114 (1952).

24. D. K. Coles and R. H. Hughes, "Microwave Spectrum of CF_3Cl," Physical Review 76, 858 (1949).

25. J. Sheridan and W. Gordy, "The Microwave Spectra and Molecular Structures of Trifluoromethyl Bromide, Iodide and Cyanide," Journal of Chemical Physics 20, 591-595 (1952).

26. J. P. Zietlow, F. F. Cleveland, and A. G. Meister, "Raman Spectra, Assignments and Force Constants for Some Trichloromethanes," Journal of Chemical Physics 18, 1076-1080 (1950).

27. C. E. Decker, A. G. Meister, and F. F. Cleveland, "Force Constants and Calculated Thermodynamic Properties for Some Trifluoromethanes," Journal of Chemical Physics 19, 784-788 (1951).

28. H. B. Weissman, R. B. Bernstein, S. E. Rosser, A. G. Meister, and F. F. Cleveland, "Infrared Spectral Data, Rotational Constants, Normal Coordinate Treatments, and Thermodynamic Properties for CD_3Br and CH_3Br," Journal of Chemical Physics 23, 544-551 (1955).

29. Private communications from Dr. J. M. Dowling, Arizona State University, Tempe, Arizona (1961).

30. P. F. Fenlon, F. F. Cleveland, and A. G. Meister, "Vibrational Spectra, Force Constants, and Calculated Thermodynamic Properties for CH_3I and CH_3D," Journal of Chemical Physics 19, 1561-1565 (1951).

31. P. R. McGee, F. F. Cleveland, A. G. Meister, and C. E. Decker, "Infrared Spectral Data, Assignments, Potential Constants, and Calculated Thermodynamic Properties for CF_3Br and CF_3I," Journal of Chemical Physics 21, 242-246 (1953).

32. P. N. Wolfe, "Microwave Spectrum of Chloroform," Journal of Chemical Physics 25, 976-981 (1956).

33. M. Cowan and W. Gordy, "Millimeter and Submillimeter Wave Spectroscopy: Evaluation of Centrifugal Distortion Effects in BrCN and NF_3," Bulletin of the American Physical Society, Washington, D. C., 25 April 1960, p. 241.

34. M. W. Long, Microwave Spectrum of Fluorotrichloromethane, Unpublished Ph.D. Thesis, Georgia Institute of Technology, June 1959, p. 75; also available in form of T.R. No. 1, Contract No. Nonr-991(07), Armed Services Technical Information Agency No. 216615, June 1959.

35. W. Low and C. H. Townes, "Molecular Dipole Moments and Stark Effects," Physical Review 76, 1295-1299 (1949).

36. Townes and Schawlow, op. cit., p. 250.

37. J. M. B. Kellog, I. I. Rabi, and N. F. Ramsey, "An Electrical Quadrupole Moment of the Deuteron," Physical Review 57, 677-695 (1940).

38. Townes and Schawlow, op. cit., p. 251.

39. C. C. Costain, "Microwave Spectrum and Molecular Structure of Methylchloroacetylene," Journal of Chemical Physics 23, 2037-2041 (1955).

40. A. Davis, F. F. Cleveland, and A. G. Meister, "Vibrational Spectra, Potential Constants, and Calculated Thermodynamic Properties for Dibromodichloromethane," Journal of Chemical Physics 20, 454-459 (1952).

VITA

Richard Clayton Johnson was born on May 9, 1930, in Eveleth, Minnesota, the son of Elvin and Sadie E. Johnson. He was married to Miss Sallie S. Hairston in 1958, and they presently have one daughter, Karen Louise.

He received his secondary education in Orlando, Florida, graduating from Orlando Senior High School in 1948. He entered the Georgia Institute of Technology in the fall of 1948, and received the degree of Bachelor of Science in Physics in 1953. During his undergraduate years, he worked part time as a co-operative student for the Georgia Power Company, as a laboratory instructor for the School of Physics, and as a technician for the Engineering Experiment Station of the Georgia Institute of Technology.

During the summer of 1953, he worked as a Research Assistant for the Engineering Experiment Station. In the fall of that year, he entered the U. S. Navy where he attended the Naval Electronic Materiel School at Treasure Island, and served as Electronics Officer aboard the U. S. S. Moale (DD 693). He was released from active duty in the fall of 1955, and at present he is a Lieutenant in the U. S. Naval Reserve.

In 1956, Mr. Johnson was employed by the Engineering Experiment Station of the Georgia Institute of Technology, and he began graduate work in the School of Physics. He is currently a Research Physicist with the Engineering Experiment Station.